THE EXPERIMENTAL INVESTIGATION OF THE TEMPERATURE DEPENDENCE OF NOISE IN GERMANIUM P-N JUNCTIONS

by

WINSTON R. SAMAROO

Submitted in partial fulfillment of the requirements
for the degree of Master of Science

Department of Electrical Engineering,
Faculty of Pure and Applied Science,
The University of Ottawa,
Ottawa, Canada,
1961.

ACKNOWLEDGMENTS

My thanks are due to Professor O. Celinski for introducing me to the subject of "Noise-Measurements" and for his interest and help throughout this research project. I have received many helpful suggestions from the members of the Electrical Engineering and Physics Departments and for these I am also thankful.

Financial assistance was received from the National Research Council through grant number A-871, and this is gratefully acknowledged.

PART II

EXPERIMENTAL RESULTS AND CONCLUSIONS

LIST OF PRINCIPAL SYMBOLS

df: an interval of frequancy.

e: base of Naperian logarithms.

$\overline{e^2}$: mean square noise voltage.

f: frequency.

f_o: resonant frequency.

G: voltage gain.

g_m: transconductance of a vacuum tube.

I: diode current, positive from p to n.

I_o: reverse saturation current of a p-n junction.

$\overline{i^2}$: mean square noise current.

j: $\sqrt{-1}$.

k: Boltzmann constant, 1.38×10^{-23} joules per Kelvin degree.

N: noise factor.

N_{R_a}: output thermal noise power due to resistance R_a.

q: electron charge, 1.602×10^{-19} coulombs.

r_p: plate resistance of a vacuum tube.

T: temperature in degrees Kelvin.

$\omega_o = 2\pi f_o$ = resonant angular frequency.

$\omega = 2\pi f$ = angular frequency.

μ = amplification factor of a vacuum tube.

CHAPTER 1: INTRODUCTION

The study of the temperature dependence of noise in p-n junctions had its origin in O. Celinski's[1] work on a noise thermometer. One of the objectives of that work was to find out if transistors could be used at liquid helium temperatures for amplifying thermal noise generated in a resistor. This question still remains unanswered, one of the reasons being the lack of adequate knowledge of the behaviour of p-n junctions at low temperatures both in its d-c and a-c aspects. The investigation of the behaviour of the temperature dependence of p-n junctions was arbitrarily divided into two questions i) the temperature dependence of current-voltage characteristics of p-n junctions and ii) the temperature dependence of noise (charge fluctuations) generated within the junction.

These two problems are very closely related and should have been investigated simultaneously, however, due to practical limitations and greater appeal of the latter, the investigation of noise was given temporary preference.

It is expected that the investigations of p-n junction noise temperature dependence will prove to be of wider interest and significance than only the application in noise thermometry. P-N junctions are microscopically complex solid state devices and a knowledge of their noise properties might become one more tool for probing into the unknown or

for confirming uncertain theories.

A possible engineering aspect of this investigation might be a method for testing the quality of p-n junctions in diodes and transistors, since the noise behaviour of p-n junctions is related to their performance and reliability[2].

This thesis describes the construction and assembly of noise-measuring equipment, treats special problems during the assembly and presents the results obtained for the noise of a germanium junction measured as a function of forward[a] bias current at the temperatures of 4.2°K (boiling point of helium), 80°K (boiling point of nitrogen) and 300°K (room temperature).

Part I, consisting of chapters 2 to 4, is devoted to a description of the experimental apparatus. The bulkier parts of the equipment, the preamplifier, amplifier and power supplies are described in chapter 2; chapter 3 deals with the circuit for measuring the output voltage from the noise-amplifier, while chapter 4 treats the important details concerning the circuitry at the input to the preamplifier. These circuits were used to connect the p-n junction to the preamplifier, to bias the p-n junction, to measure the small signal a-c impedance (hereafter called incremental resistance.

---

a) "forward" implies a flow of conventional current from p-region to n-region through the junction.

see section 5.1) of the junction and to calibrate the voltage gain of the noise-measuring equipment.

Part II, chapters 5 and 6, presents experimental results and their significance.

The samples used were the collector-base junctions of Philco 2N393 p-n-p micro-alloy germanium transistors; and the characteristics of these junctions are described in section 5.1. The rest of chapter 5 presents the results of noise measurements made about a centre frequency of 1 mc at which frequency I assumed that flicker[b] noise was negligible. In chapter 6, the experimental results are compared with existing theory.

The specifications of the noise-measuring equipment and its block diagram (figure 1.1) are given in the following two pages.

---

b) Flicker noise is a convenient term describing any noise having a spectral density proportional to f^{-a}, where "f" is the frequency, and "a" is close to unity.[3,4] The effect of flicker noise becomes trivial above a few kilocycles for relatively pure semiconductor materials, but an appreciable effect may exist up to 1 mc for impure materials.[4,5,6]

SPECIFICATIONS OF THE EQUIPMENT

Overall voltage gain	122 db ± 0.5 db
Frequency of operation	1.150 mc ± 1.5 kc
Equivalent bandwidth[c]	4.5 kc ± 0.2 kc
Stability over a 24 hour period	0.75%
Input noise-voltage range	10 mμv - 0.5 μv
Accuracy at maximum sensitivity	5%

---

c) Equivalent bandwidth is defined as

$$\Delta f_e = \frac{\int_0^\infty G(f)\, df}{G_m}$$

where $G(f)$ is the power gain of the amplifier and G_m is the maximum gain, i.e. Δf_e is the width of a rectangle whose area is the area under the frequency response curve of the amplifier, the height of the rectangle being equal to the maximum gain. In the case of a superheterodyne receiver, this includes image frequency and spurious responses. Hereafter Δf_e will be simply written df.

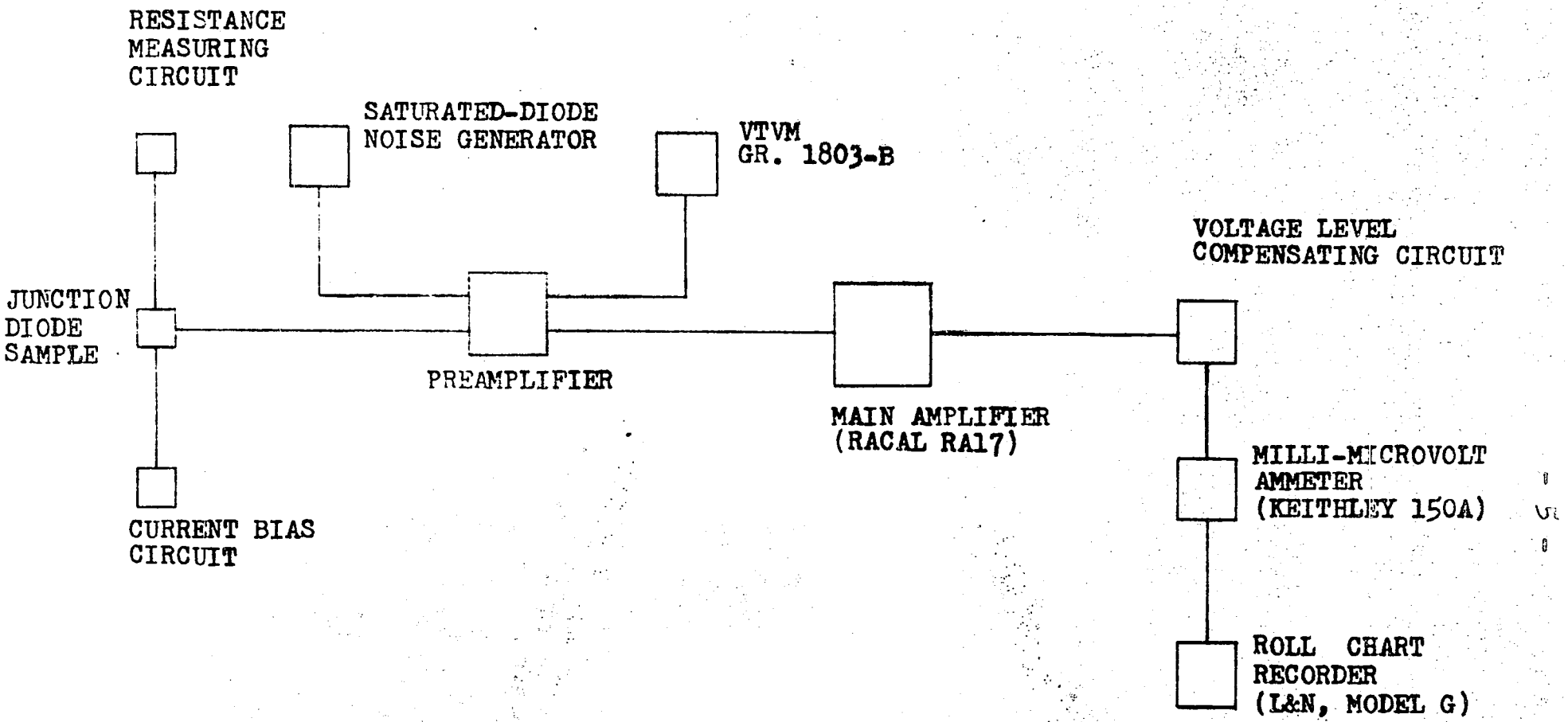

FIGURE 1.1

BLOCK DIAGRAM OF NOISE-MEASURING EQUIPMENT

PART I

THE EXPERIMENTAL APPARATUS

CHAPTER 2: NOISE AMPLIFIER

2.1 Cascode Preamplifier

The noise voltage expected from a p-n junction operating under normal forward bias conditions ranges from about 10^{-9} to 10^{-6} volts as calculated from van der Ziel's[4] model of a p-n junction (figure 6.1). Since the gain of the main amplifier (80 db) was not sufficient to raise the noise signal to a suitable level for measurement, a cascode pre-amplifier was built to provide additional gain and at the same time reduce the overall noise factor of the noise-amplifier.

The noise factor of a chain of amplification stages of available gains G_1, G_2, G_3, ---- and corresponding noise factors N_1, N_2, N_3, ---- is given[7] by

$$N_o = N_1 + \frac{N_2-1}{G_1} + \frac{N_3-1}{G_1G_2} + \text{----} \qquad (2.1)$$

If, therefore, the first stage of the chain has a high gain, the second and subsequent terms of (2.1) are negligible and N_o becomes approximately equal to N_1. This first stage may be designed to have a low noise factor. The cascode amplifier devised by H. Wallman, A. B. Macnee and C. P. Gadsen[8] in 1944 satisfies both the above requirements and therefore is suitable for use as the first stage of a chain of amplification stages.

A pentode amplifier has a high gain but also a high noise factor due to partition noise[a]. A triode amplifier has a low noise factor but a low gain. The cascode amplifier, however, consisting of a grounded cathode triode followed by a grounded grid triode has the high gain and stability of a pentode and the low noise factor of a triode.

Figure 2.2a shows the a-c circuit of a cascode amplifier and figure 2.2b shows its piecewise linear equivalence. From (2.2b) it may be shown that the voltage gain of the cascode amplifier is given by

$$G = \frac{\mu_1(\mu_2+1)\, R_L}{(\mu_2+1)r_{p1}+R_L+r_{p2}} \qquad (2.3)$$

where μ's are amplification factors, r_p's are plate resistances and R_L is the load resistance of the second tube.
If $\mu_1 = \mu_2$, $r_{p1} = r_{p2}$, (both tubes are operated under the same conditions) and $(\mu+2)r_p \gg R_L$ then (2.3) reduces to

$$G = g_{m1}R_L \qquad (2.4)$$

where g_m is the transconductance of the tubes. Equation 2.4, however, gives the gain of a pentode amplifier.

---

a) Partition noise is caused by the random division of cathode current between plate and screen grid of a tube.

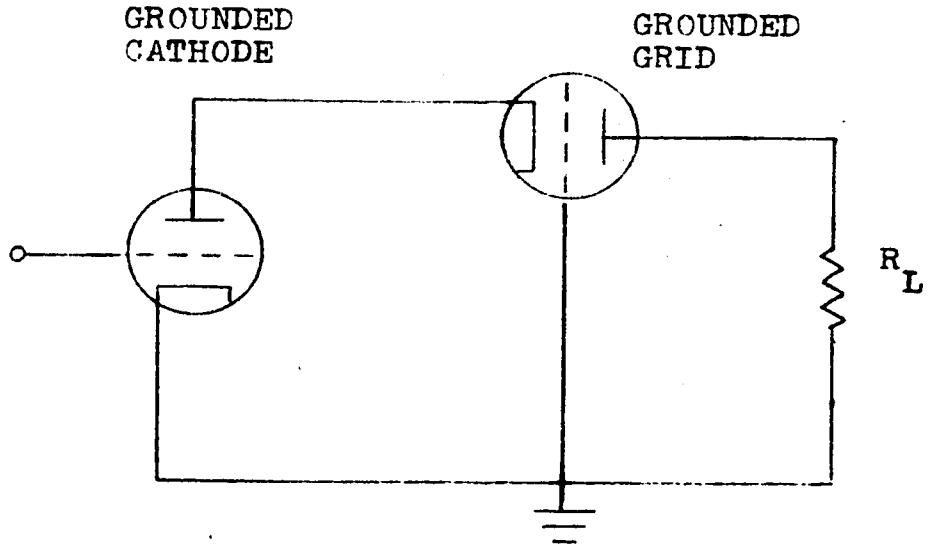

2.2a A-C CIRCUIT OF A CASCODE AMPLIFIER AT LOW FREQUENCIES

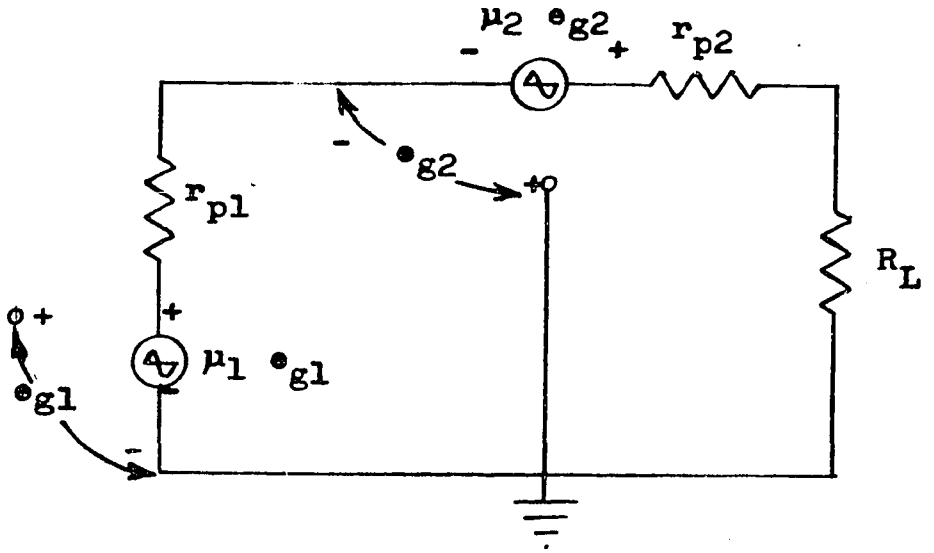

2.2b PIECEWISE LINEAR EQUIVALENCE OF CASCODE AMPLIFIER

FIGURE 2.2

The gain (G_1) of the first tube of the cascode amplifier is about unity (for the above assumption, $\mu_1 = \mu_2$, $r_{p1} = r_{p2}$, and $(\mu+2)r_p \gg R_L$, $G_1 = \frac{R_L+r_p}{r_p}$), therefore this portion of the amplifier is stable. Since the grid of the second tube is grounded, it acts as a screen for the plate to cathode feedback path and therefore a large gain may be achieved in this tube with good stability. In this respect the second tube resembles a pentode. These two factors account for the stability of the cascode amplifier.

Using the approximation that the equivalent noise resistance[b] of a triode is given by

$$R_{eq} = \frac{2.5}{g_m} \tag{2.5}$$

It can be shown (cf. W. R. Bennett[9]) that the noise factor of a triode is given by

$$N_t = 1 + \frac{2.5}{g_m R_s} \tag{2.6}$$

and that of a cascode amplifier by

$$N_c = 1 + \frac{2.5}{g_{m1} R_s} + \frac{2.5}{g_{m1}^2 g_{m2} R_{p1}^2 R_s} + \frac{1}{g_{m1}^2 R_L R_s} \tag{2.7}$$

where R_s is the source resistance.

---

b) The equivalent noise resistance is that resistance, which when placed in the grid circuit of a "noiseless tube", produces the same mean square noise current in the plate circuit as the tube.

Since the last two terms in (2.7) are small, the noise factor of the cascode amplifier is only slightly greater than that of a triode, given by (2.6) (this will be shown to be the case for the experimental preamplifier).

The cascode preamplifier (figure 2.8) was built using two Philips 6688 tubes, chosen because of their high g_m's and therefore low equivalent noise resistance. The tubes were operated so that $\mu_1 = 7$, $r_{p1} = 500\Omega$, $g_{m1} = 14{,}000\mu\mho$, $\mu_2 = 37$, $r_{p2} = 10K\Omega$ and $g_{m2} = 3{,}700\mu\mho$. This gave an experimental gain of 42 db and a calculated gain of 37 db (using equation 2.3), the discrepancy occuring because the tube constants were estimated graphically from the E_p vs I_p characteristics.

When the tube constants and an average value of the source resistance (500Ω) are substituted in (2.7) the result is

$$N_c = 1 + 0.35 + 0.034 + 0.001$$

showing that the last two terms in (2.7) are small and that the noise factor is approximately 1.4. Figure 2.8 also shows the cathode follower used to provide a low output impedance to feed the main amplifier.

2.2 Main Amplifier

The bulk of the amplification was provided by a Racal communication receiver (RA-17), which was operated with

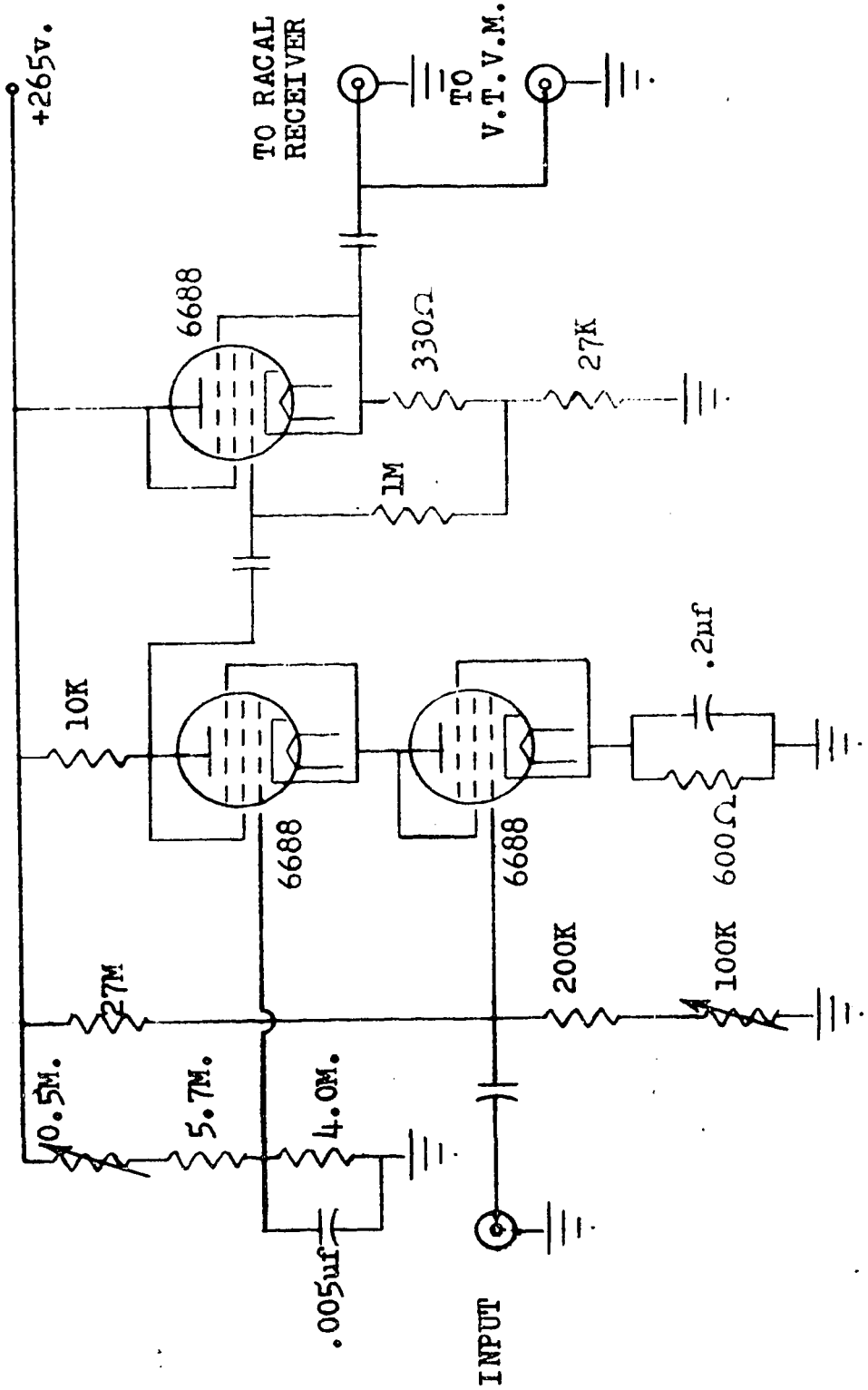

FIGURE 2.8

THE CASCODE PREAMPLIFIER

the controls set at "wide-band" antenna tuning, "minimum" antenna attenuation, AVC "off" and the IF gain control adjusted to give the largest output without a noticeable distortion. A center frequency about 1 mc was chosen which was high enough to consider flicker noise negligible and at the same time low enough to enable the use of lumped circuit consideration. The exact figure was 1.15 mc because at this frequency there was not much disturbance from RF transmitters.

The variable band-width control of the receiver was set at 8 kc, at which setting the equivalent bandwidth was measured to be 4.5 kc. The equivalent bandwidth was determined by plotting the frequency response curve (power gain versus frequency) and constructing a rectangle equal in area to the area under the curve with the height of the rectangle equal to the maximum gain. The width of the rectangle was the equivalent bandwidth (figure 2.9). The image response in the receiver is rated to be suppressed 60 db.

The output from the receiver was taken from the available "RF level" connections to the "s" meter in the receiver. Figure 2.10 shows the detector diode, the RF filter and the "RF level" leads which are connected across a portion of the load resistor of the diode detector. Up to this point the measured gain of the receiver was 80 db.

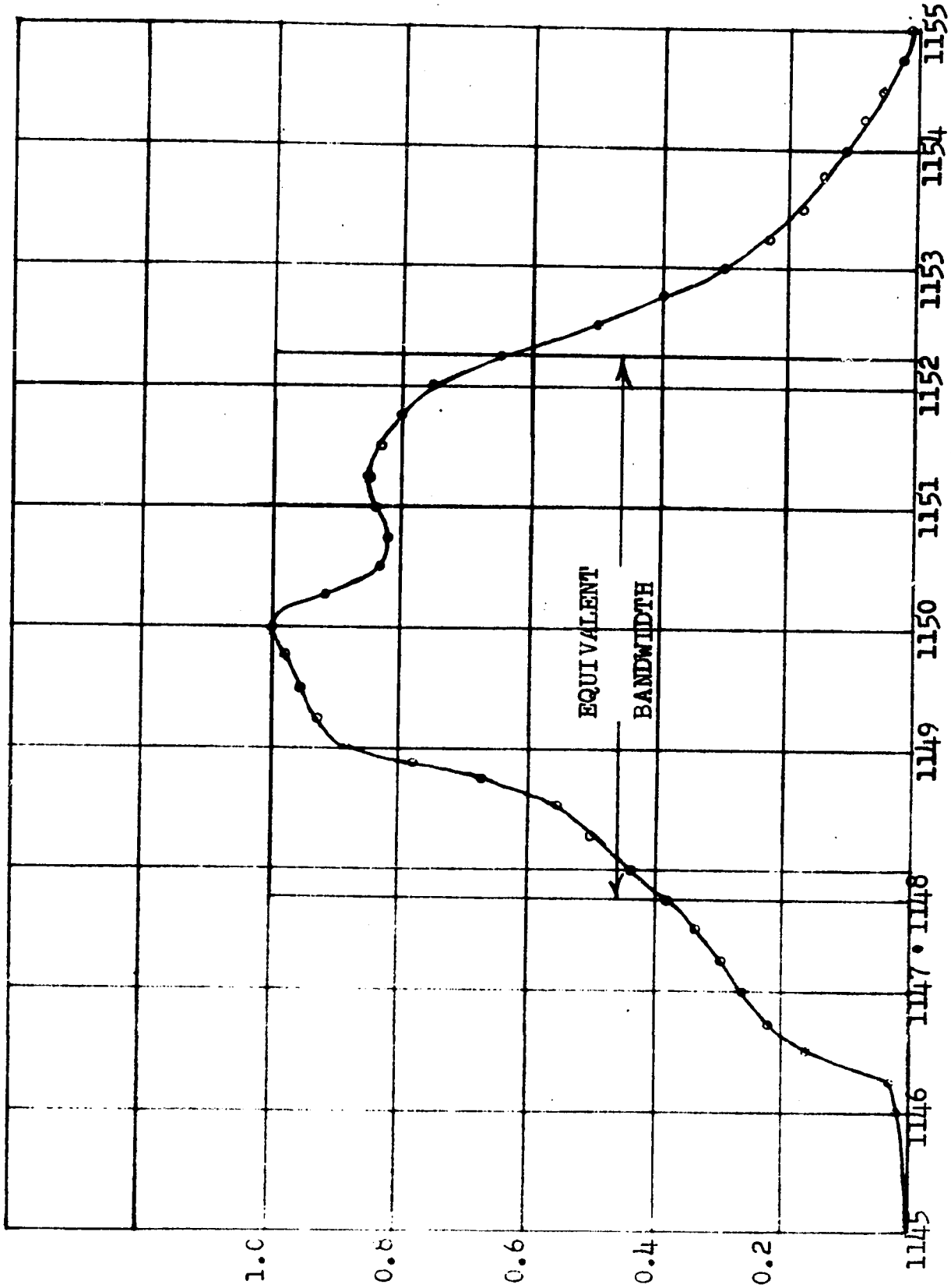

FIGURE 2.9

FREQUENCY RESPONSE OF NOISE-AMPLIFIER

WITH EQUIVALENT BANDWIDTH SHOWN

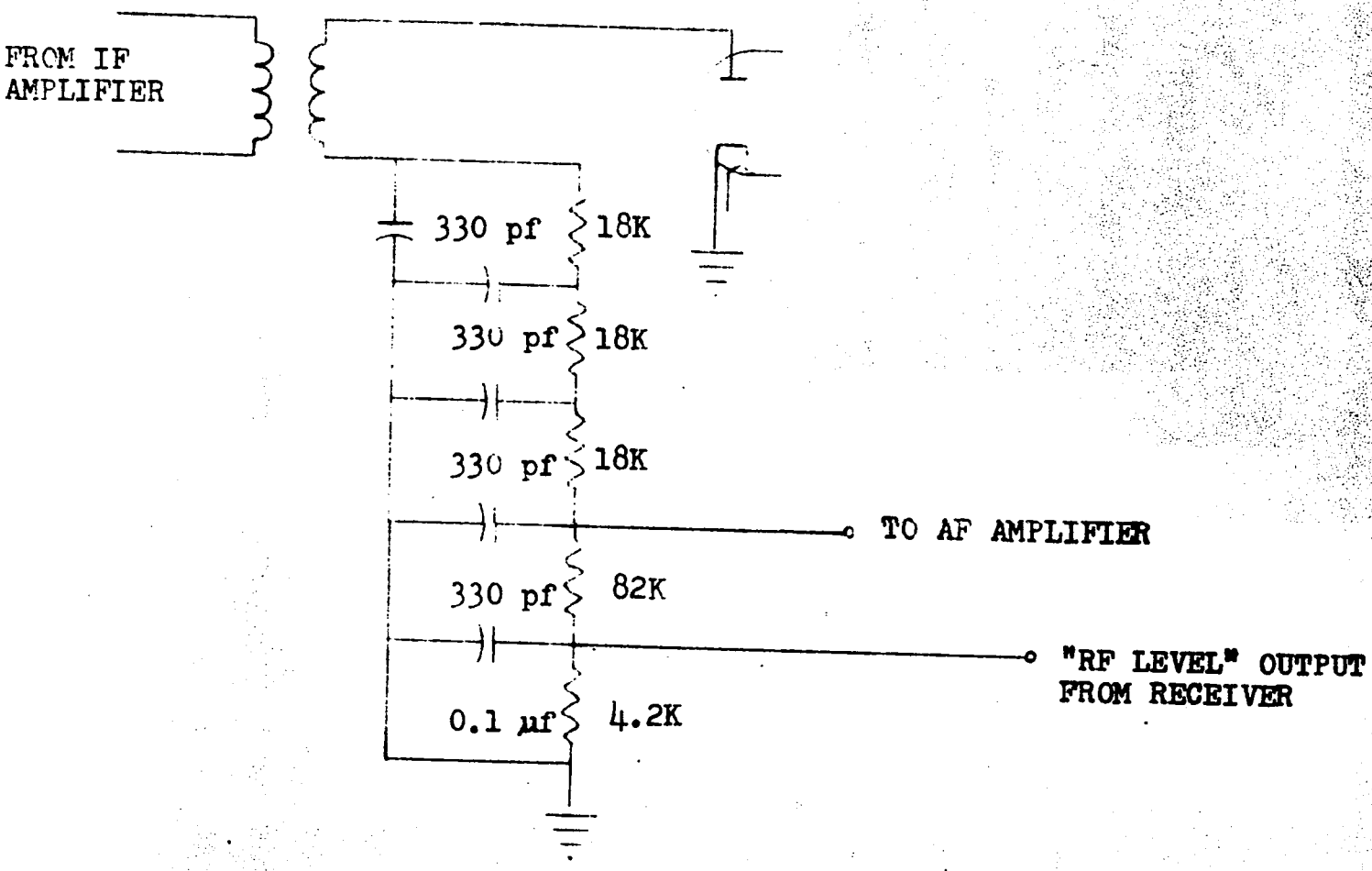

FIGURE 2.10

DETECTOR STAGE SHOWING OUTPUT FROM

THE RACAL RECEIVER

2.3 Power Supplies and stability

Power to the entire equipment was supplied by an a-c regulated power supply (Sorensen 1001) with a rated regulation accuracy of 0.01% and a response time of 0.1 seconds. The regulation accuracy was checked by rectifying the output from two similar Sorensen regulators and recording the difference in output voltage on a roll chart recorder. One of the regulators was left undisturbed while the other was subjected to changes from no-load to full-load and ± 10% changes in line voltage. The response was within the rated regulation accuracy. Since the load on the power supply was constant, the power supply was used principally to make the equipment independent of line fluctuations. Because the equipment needed three hours to achieve thermal equilibrium, a time switch was used with the a-c regulator allowing a 24 hour "ON-OFF" programming.

The unregulated power supply of the Racal receiver was replaced by a regulated d-c supply. The d-c supply was fed from the a-c regulator and gave a stability of 0.025%, which was checked over a period of 24 hours.

The stability of the entire noise-measuring equipment was 0.75%. This was measured by feeding into the preamplifier a constant noise voltage (thermal noise from a resistor) and recording the output from the amplifier over a period of 24 hours.

CHAPTER 3: OUTPUT CIRCUITS

3.1 Voltage Compensating Circuit

The output voltage from the receiver due to the background noise of the amplifier (shorted input terminals) was 0.5v. while the output voltage due to the source ranged from 5mv. to 1v. In order to measure the small incremental d-c voltage (the difference between short-circuited input terminals and the noise source connected to the input terminals) a voltage level compensating circuit was used to keep the pointer of the output meter "on-scale" on sensitive ranges.

As shown in figure 3.1, a variable voltage of opposite polarity and approximately equal to the receiver output voltage at shorted input terminals, was added to the receiver output voltage. The voltage recorded on the output meter was therefore the difference between the receiver output and the voltage from the compensating circuit allowing small incremental voltage to be measured. The impedance of the compensating circuit was designed small ($400 \pm 75\ \Omega$) in comparison to the input impedance of the output meter ($90 M\Omega$) and therefore introduced less than 0.01% error in any measurement. The purpose of the sliding contact "c" shown in figure 3.1, is best explained in conjunction with the recorder (sec. 3.2)

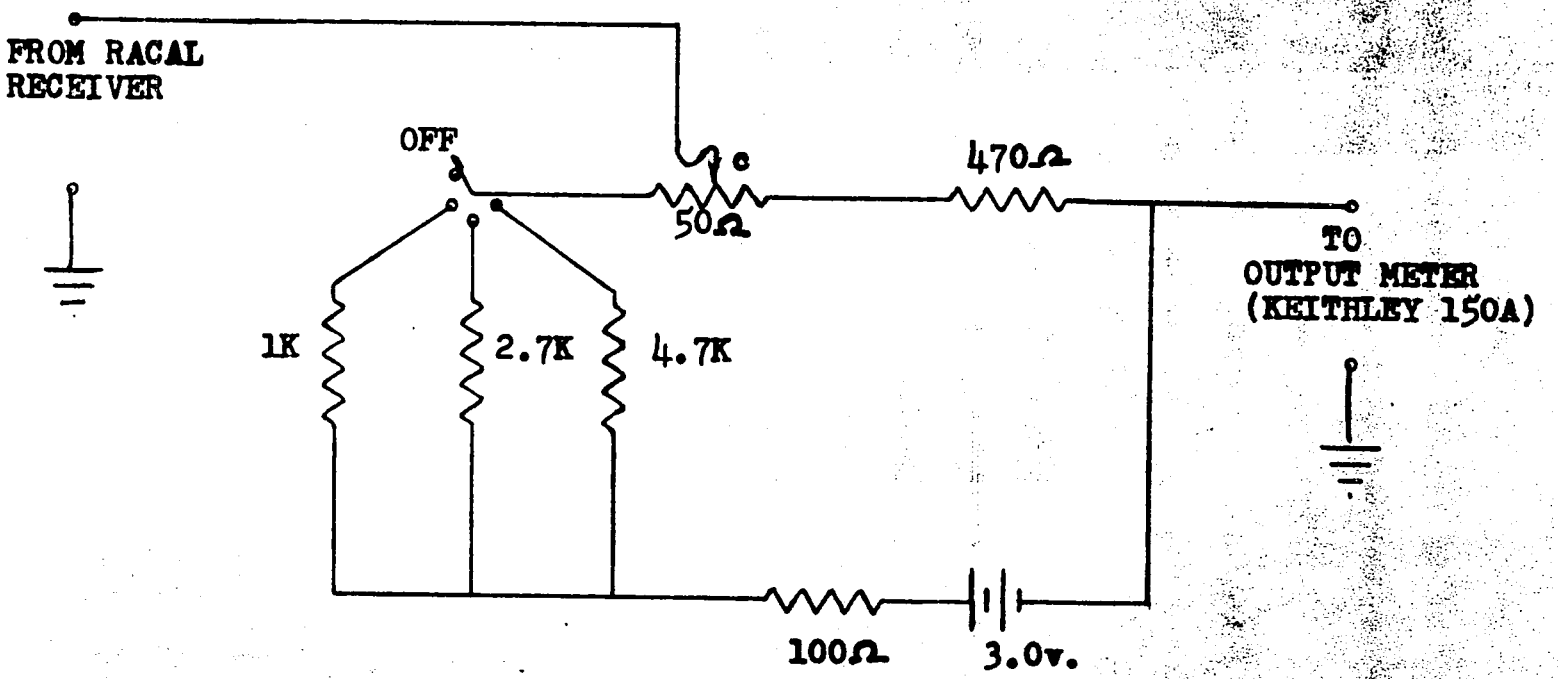

FIGURE 3.1

VOLTAGE COMPENSATING CIRCUIT

3.2 Output Meter and Recorder

The output meter was a micro volt-ammeter (Keithley 150A) with 13 overlapping ranges in 1x and 3x steps from one microvolt to one volt on a zero-centre scale. The meter had a rated accuracy of two per cent of full scale on all ranges and a response time of one second. The output from the Keithley meter was fed to a Leeds and Northrup roll chart recorder (model G) for keeping a permanent record of the output voltage.

At the input to the preamplifier a relay was provided for alternately shorting the input terminals and connecting the noise source to the preamplifier; this gave a record of any changes in the background noise of the amplifier, which were corrected for by this switching method. Switching was done automatically every three minutes by means of a rotating cam operating a microswitch which supplied voltage to the relay. The cam was mounted on the shaft of an a-c motor which was isolated from the input circuitry to eliminate effects from the rotating fields of the motor. Since three or four cycles of switching were allowed for each condition of the junction, the manual adjustment of parameters (diode current, meter scale, etc.) was only necessary every 18-24 minutes.

Figure 3.2 illustrates the results obtained on the recorder by the use of the above technique. These results were obtained for the noise of a sample junction at $4.2^{\circ}K$ through which different currents were flowing. The ordinate

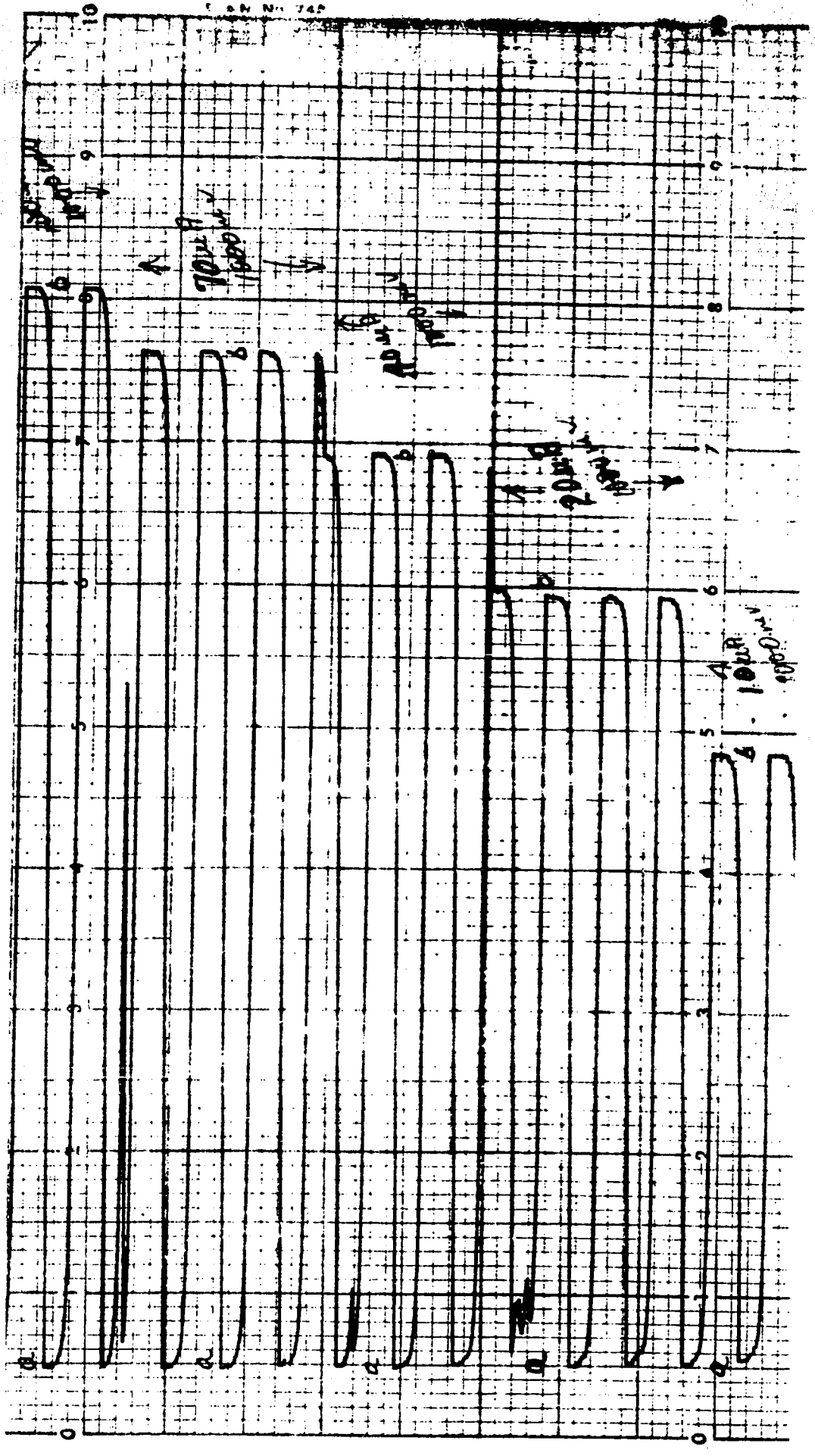

FIGURE 3.2

EXAMPLE OF THE READINGS OBTAINED ON THE RECORDER FOR COLLECTOR BASE JUNCTION OF A 2N393 TRANSISTOR AT 4.20K. THE BIAS CURRENTS AND FULL SCALE VOLTAGE RANGE ARE INDICATED ON THE DIAGRAM.

represents the time scale of four inches per hour and is of no further interest in this discussion. The abscissa represents voltage and on figure 3.2, has a full scale value of one volt. The step "a-b" is the incremental voltage due to the noise from the source, while "a" is an arbitrary zero, the position of the pointer when the input terminals to the noise-amplifier are short-circuited. The position "a" may be placed at any convenient part of the scale by adjusting the sliding contact "c" shown on figure 3.1.

CHAPTER 4: INPUT CIRCUITS

4.1 Connection of the P-N Junction to the Preamplifier

The p-n junction, whose noise properties were being investigated, was mounted at the end of a three-foot german-silver[a] tube. This permitted the immersion of the sample into a liquid helium transport vessel (figure 4.1) for low temperature measurements.

Figure 4.2 shows three different ways in which the p-n junction may be connected to the preamplifier. Of these configurations, the "Direct Connection" (Figure 4.2a) was finally used because of its simplicity. To evaluate this choice, expressions for the voltage transfer ration and the noise factor are derived and numerical values of these properties are presented in graphical form in appendix 1.

---

a) An alloy (40-60% copper, 20-30% zinc and 10-30% nickel) known for its corrosion resistance and low thermal conductivity of 0.07 cal. sec.$^{-1}$ cm.$^{-1}$ degree centigrade^{-1}. This conductivity is lower than that of any of the constituents of the alloy (copper-1.0, zinc-0.26, nickel-0.14). German silver is used extensively in low temperature work, but is being replaced to some extent by stainless steel, where rigidity is important (thermal conductivity of stainless steel-0.12)

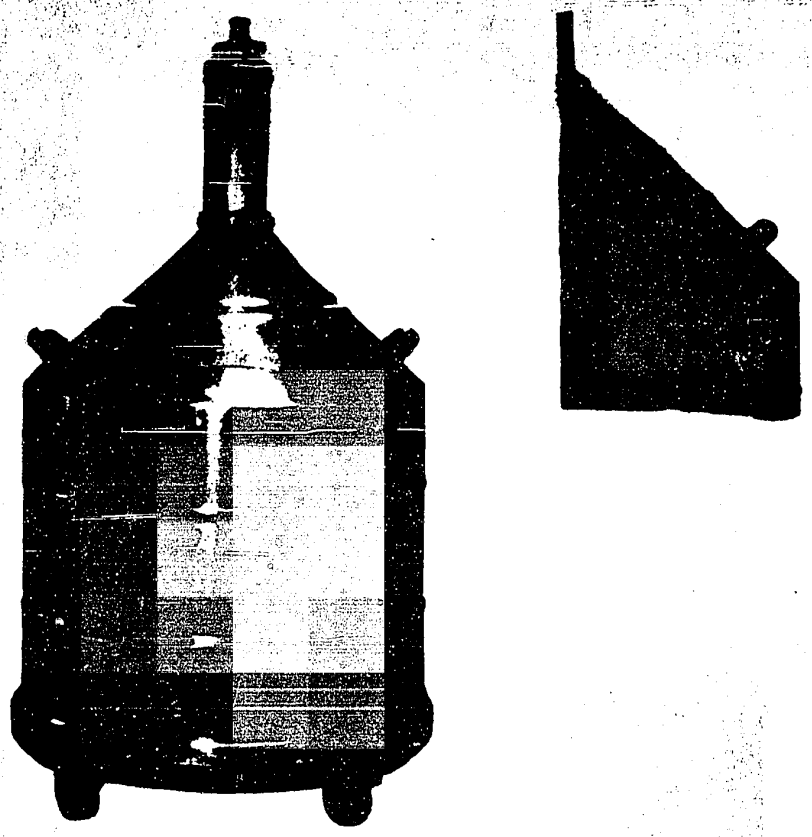

FIGURE 4.1

LIQUID HELIUM TRANSPORT VESSEL

SPECIFICATIONS: CAPACITY - 25 LITRES,

OUTER DIAMETER - 20.25", OVERALL HEIGHT 41".

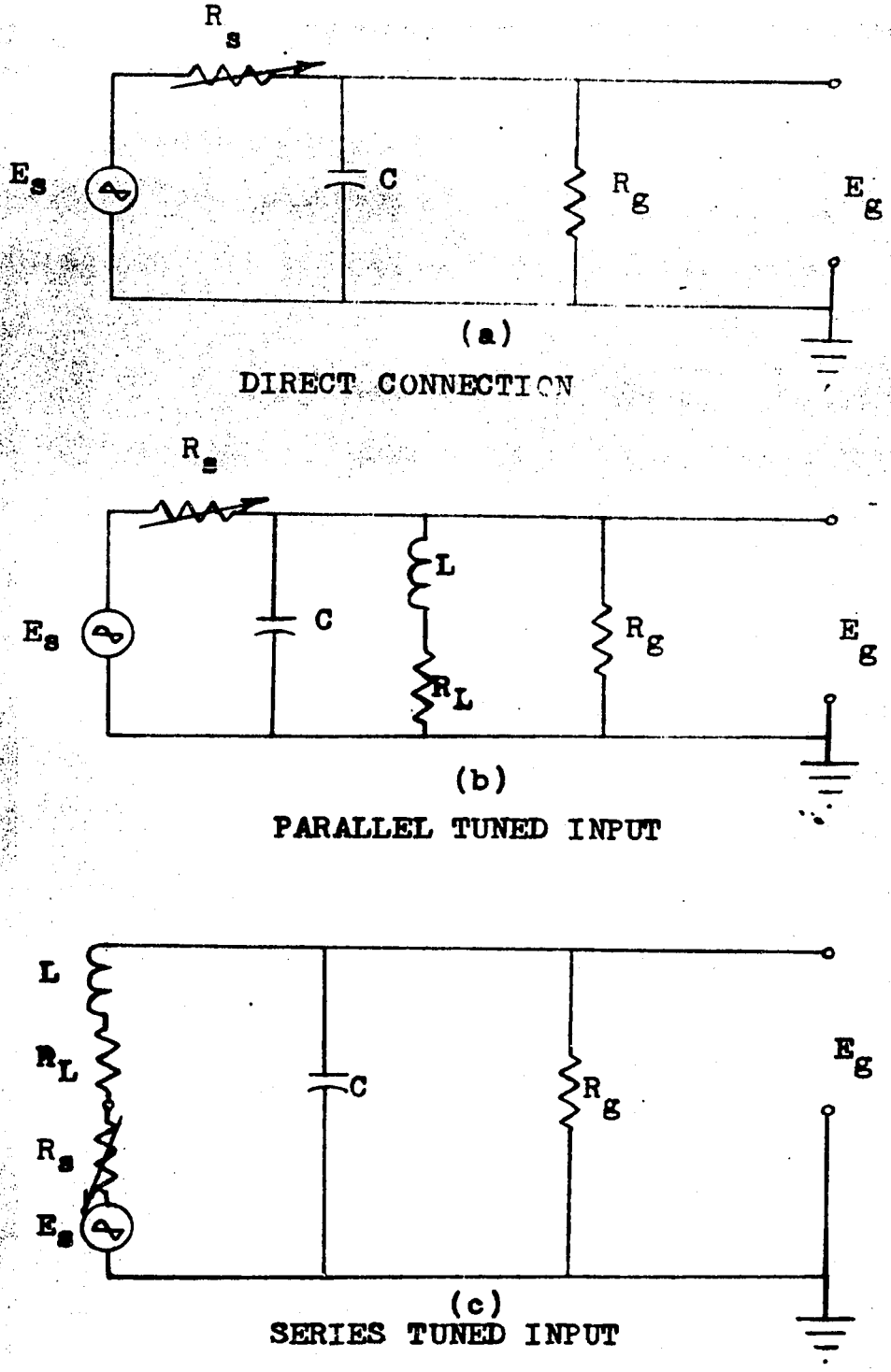

FIGURE 4.2

THREE WAYS OF CONNECTING THE P-N JUNCTION TO THE PREAMPLIFIER

E_s - voltage source, R_s - source resistance, C - stray capacitance at input to preamplifier, R_g - grid leakage resistance of first tube, E_g - voltage to grid of first tube, L tuning inductance, R_L - resistance of L.

The results of appendix 1 will now be briefly discussed with the aid of simplified expressions for the voltage transfer ratios and noise factors of the different connections (the simplified expressions are valid only for the values of the parameters listed in appendix 1).

1) Direct Connection of the p-n junction to the preamplifier (figure 4.2a) constituted a low pass R-C filter in which R_s was the incremental resistance of the junction diode, C the stray capacitance at the input to the preamplifier and R_g the grid leakage resistance of the first tube of the preamplifier. This form of connection was restricted to relatively low frequencies, because at higher frequencies the circuit attenuated the noise signal when the magnitude of R_s became comparable to the parallel impedance of R_g and C.

The voltage transfer ratio is given by (see appendix 1)[b]

$$G_1 = \frac{R_g - jR_g^2\omega C}{R_s(\omega^2 C^2 R_g^2 + 1) + R_g - jR_g^2\omega C} \qquad (4.3)$$

Where ω is the frequency of operation.
Since in this case

$$\omega C = 1.25 \times 10^{-3} \ll 1$$
$$R_g\omega C = 377 \gg 1$$

b) All data and equations appearing in the rest of this section are taken from appendix 1.

equation 4.3 reduces to

$$G_1 = \frac{1}{R_s \omega C - j} \qquad (4.4)$$

For R_s ranging from 10-1000Ω, G_1, as calculated from the exact expression, varies from 1.0 to 0.625. (Hereafter the range of values given for G's and N's were obtained from the exact expression for values of R_s ranging from 10-1000 Ω).

The noise factor is given by

$$N_1 = 1 + \frac{R_g}{G_1^2 R_s}\left[\frac{R_s - jR_s^2\omega C}{R_g(\omega^2 C^2 R_s^2+1) + R_s - jR_s^2\omega C}\right]^2 \qquad (4.5)$$

since $R_g \gg R_s$ and $\omega C R_s$ is of the order of unity, (4.5) reduces to

$$N_1 = 1 + \frac{R_g}{G_1^2 R_s}\left[\frac{R_s - jR_s^2\omega C}{R_g(\omega^2 C^2 R_s^2+1)}\right]^2 \qquad (4.6)$$

N_1 varies from 2.0-2.3 for the above mentioned range of R_s.

ii) The use of the parallel tuned input is the most elegant form of connecting the p-n junction to a good noise amplifier (sufficient gain and low noise figure). This configuration allows measurements to be made at any practical frequency by suitably tuning out the stray capacitance.

The voltage transfer function

$$G_2 = \frac{LR_g}{R_g(L+CR_LR_g)+LR_g} \qquad (4.7)$$

Where L was the inductance used for tuning out the capacitive reactance and R_L the resistance of the inductor.

Since $R_g(L+CR_LR_g) \ll LR_g$

G_2 reduces to unity

The noise factor

$$N_2 = 1 + \frac{R_s}{R_g}\left[\frac{R_g(L+CR_LR_g)+R_g}{R_g(L+CR_LR_g)+R_s}\right]^2 +$$

$$+ \frac{R_L}{R_s}\left[\frac{R_g(L+CR_LR_g)+LR_g}{LR_g}\right]^2\left[\frac{R_s - jR_g^2\omega C}{\omega L(\omega^2C^2R_g^2+1)+R_s-jR_g^2\omega C}\right]^2 \qquad (4.8)$$

The second term on the right hand side vanishes since $R_g \gg R_s$. $R_L < R_s$, the second factor in the third term is equal to $\frac{1}{G_2^2} = 1$, and $\omega L(\omega^2C^2R_g^2+1) > R_s - jR_g^2\omega C$; therefore, the third term also vanishes and (4.8) reduces to unity.

iii) The series tuned input gives a voltage transfer function greater than unity for low values of R_g and is therefore useful where the noise amplifier does not have sufficient gain. Furthermore if the amplifier has a high noise factor, the use of this circuit improves that figure.

$$G_3 = \frac{R_g + jR_g^2\omega_o C}{(R_g+R_L)(\omega_o^2C^2R_g^2+1)+R_g} \qquad (4.9)$$

Since $R_g^2\omega_o C > R_g$ and $(\omega_o CR_g)^2 \gg 1$, (4.9) simplifies to

$$G_3 = \frac{R_g^2\omega_o C}{\omega_o^2C^2R_g^2(R_g+R_L)+R_g} \qquad (4.10)$$

G_3 ranges from 43 to 0.3

The noise factor

$$N_3 = 1 + \frac{R_L}{R_g} + \frac{L^2(R_L+R_g)^2}{R_gR_gG_3\left[CR_g(R_L+R_g)+L\right]^2} \qquad (4.11)$$

the third term on the right hand side is negligible therefore (4.11) reduces to

$$N_3 = 1 + \frac{R_L}{R_g} \qquad (4.12)$$

and ranges from 1.63 to 1.01

In using any form of tuned input the bandwidth of the input circuit must be large in comparison with the bandwidth of any tuned stages which follow.[10] This is for the convenience of having the overall bandwidth independent of variables at the input to the preamplifier (the bandwidth of the input circuit is a function of incremental resistance which is dependent on bias current and temperature). In the case of the series tuned input, this involves a compromise

between a high voltage amplification and a broad bandwidth.

Summarizing, the direct connection was used because the voltage transfer ratio was constant over a wider range of incremental resistance changes than the series tuned input and introduced less calibration difficulties. Although the parallel tuned circuit would have performed better, the direct connection was chosen in preference to the parallel tuned input because of simplicity of operation.

Since the direct connection was chosen, a curve was prepared to correct for the attenuation of noise signal at higher values of incremental resistances. The correction curve is the reciprocal of the voltage transfer ratio constructed as a function of incremental resistance. The correction curve is shown on figure 4.13, with an inserted diagram of the circuit used in obtaining the curve.

4.2 Current Bias Circuit

This circuit (figure 4.14) was designed to deliver d-c currents in the range of 10μA to 20mA to the junction. The internal impedance of the circuit was always more than 500 times the impedance of the junction and therefore introduced less than 0.2% error in any measurement.

FIGURE 4.13

CORRECTION CURVE TO CORRECT FOR THE ATTENUATION OF THE SIGNAL AT HIGH VALUES OF R_s

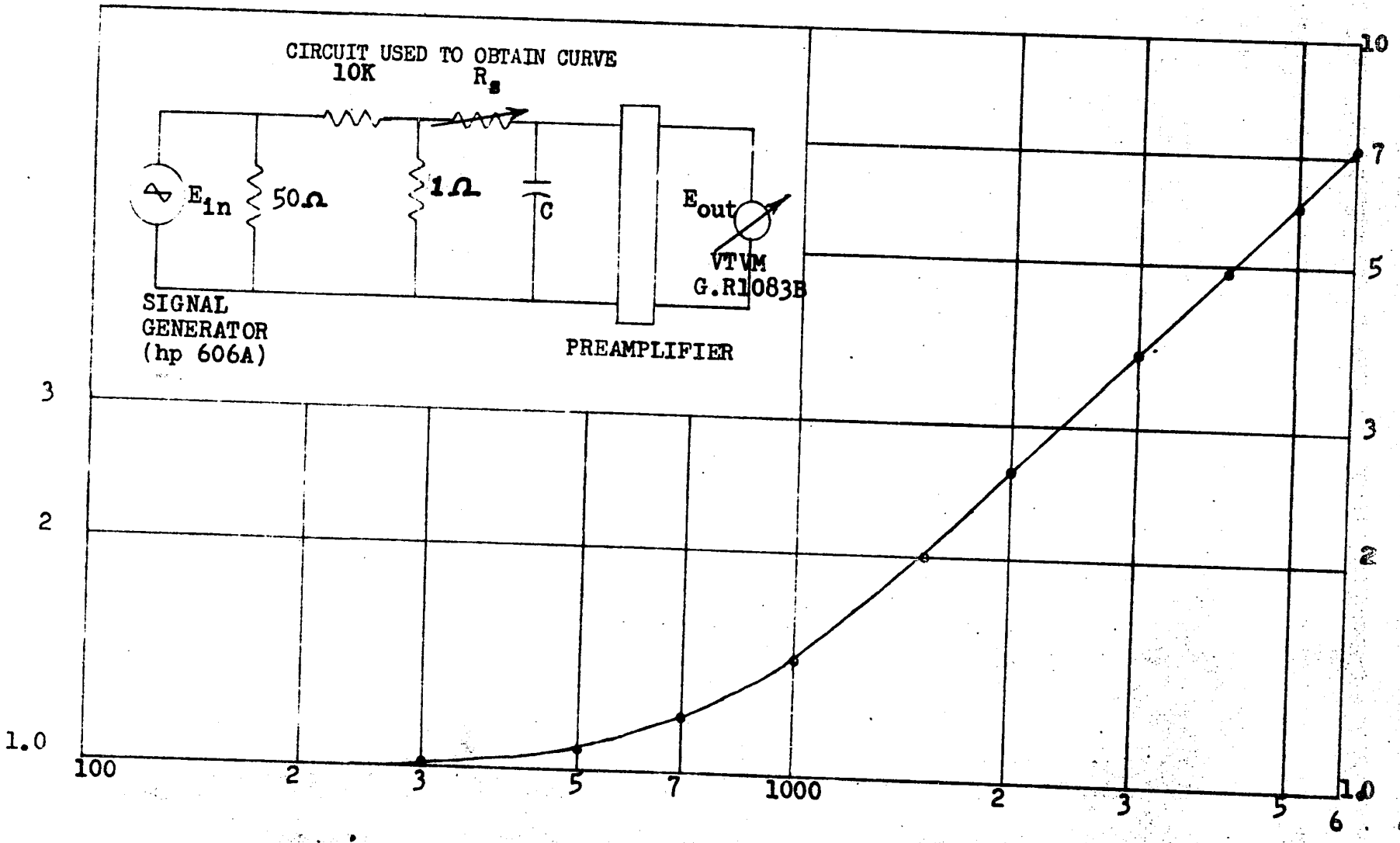

FIGURE 4.13

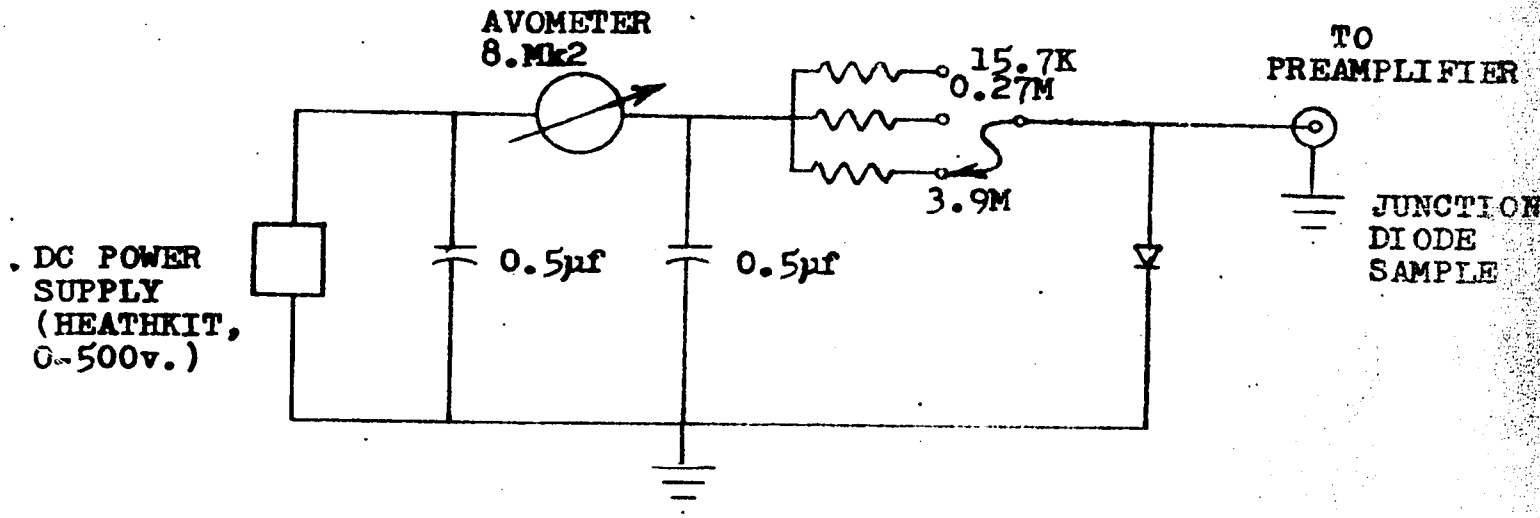

FIGURE 4.14

CURRENT BIAS CIRCUIT

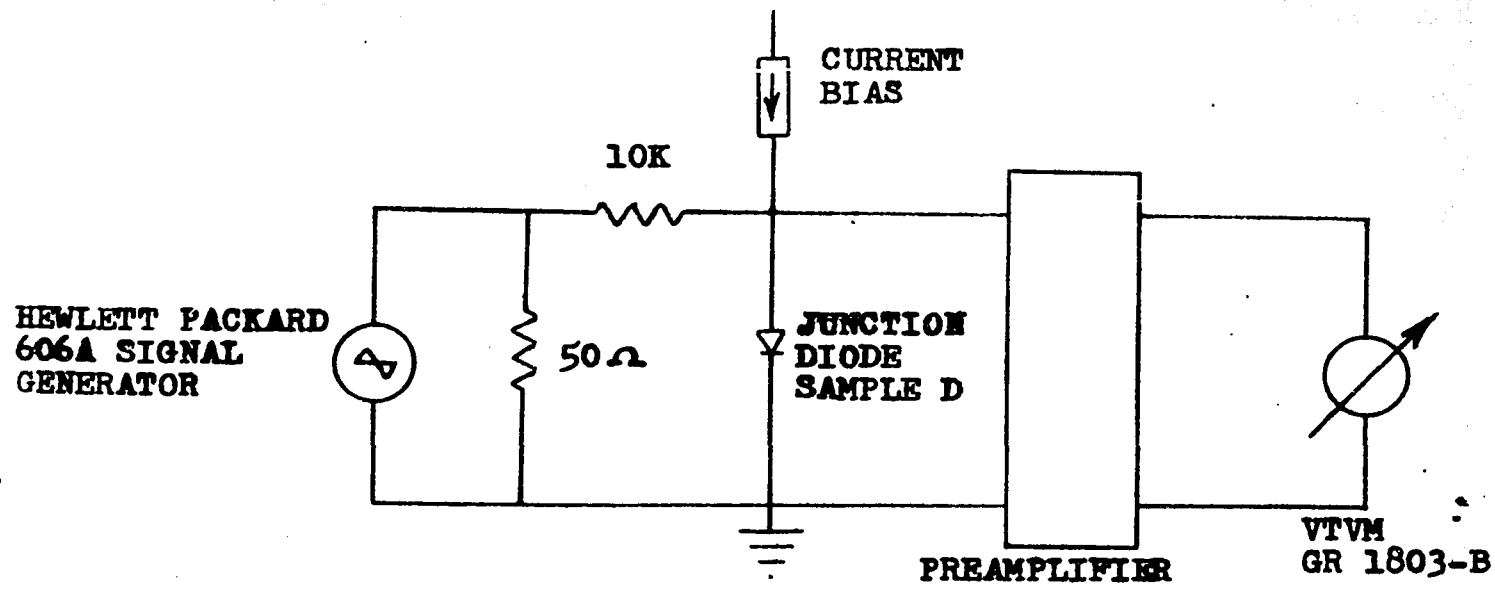

FIGURE 4.15

RESISTANCE MEASURING CIRCUIT

4.3 Resistance Measuring Circuit

Since the incremental resistance of a p-n junction is a function of bias current, additional circuitry (figure 4.15) was provided at the input of the preamplifier for determining this resistance at any bias current (cf. section 5.3). The resistance was measured by passing a known a-c current through the junction and measuring the resulting voltage.

The circuit was calibrated by substituting resistors of different values, ranging from 10-1000 Ω in the place of the junction diode D (figure 4.15) and noting the values of the signal generator voltage necessary to keep the output from the preamplifier at an arbitrarily chosen constant value (0.5v.). The calibration curve (figure 4.16) was made by plotting resistance versus the generator voltage.

4.4 Gain Calibration

The gain of the noise-amplifier was measured by applying a known noise signal at the input of the amplifier and measuring the output. As a noise-generator, a saturated[a]

---

a) The condition of a diode under which the plate current is a function only of cathode temperature, i.e. independent of plate voltage (neglecting Schottky's effect).

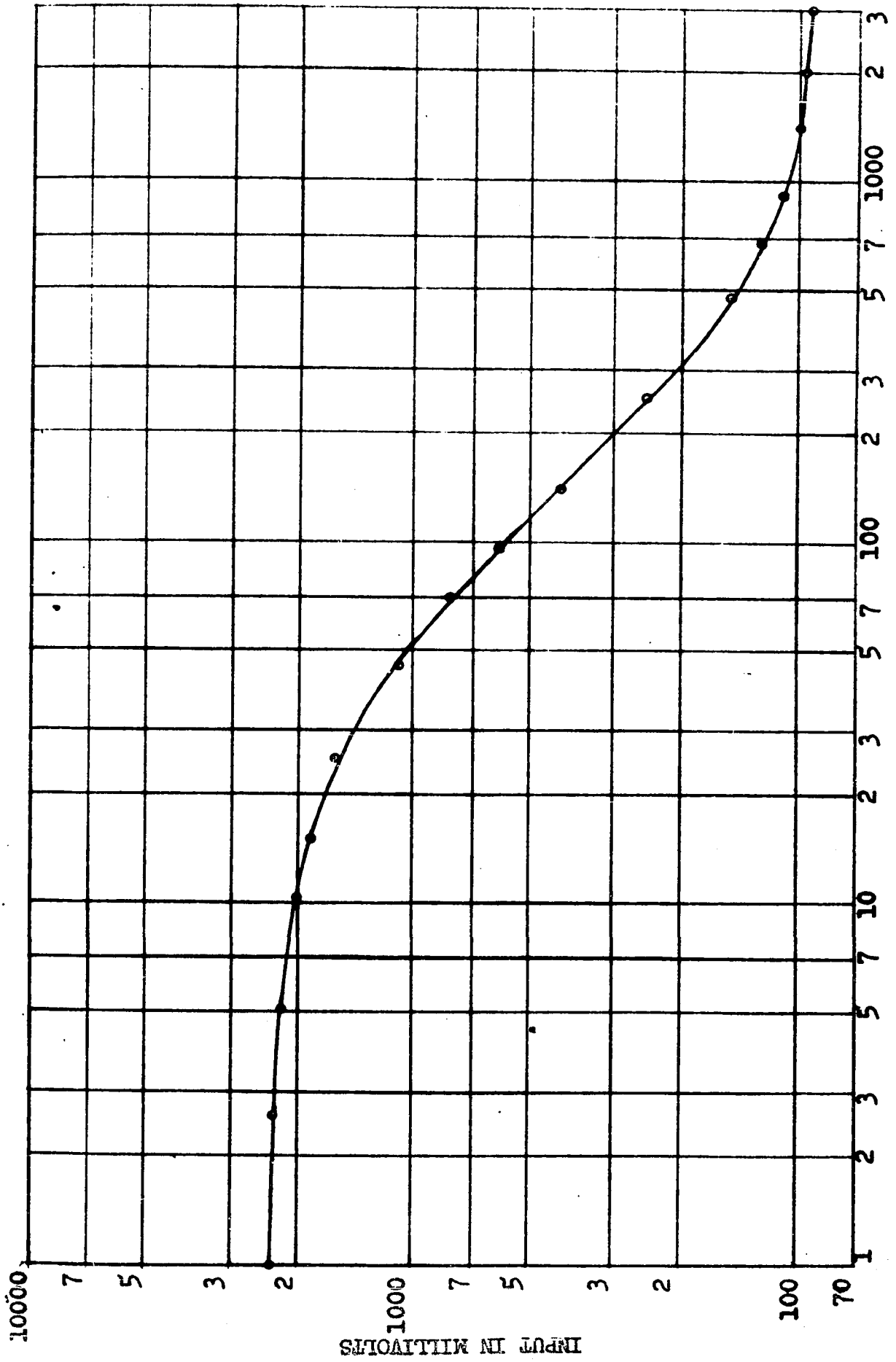

FIGURE 4.16

CALIBRATION CURVE FOR RESISTANCE MEASUREMENT

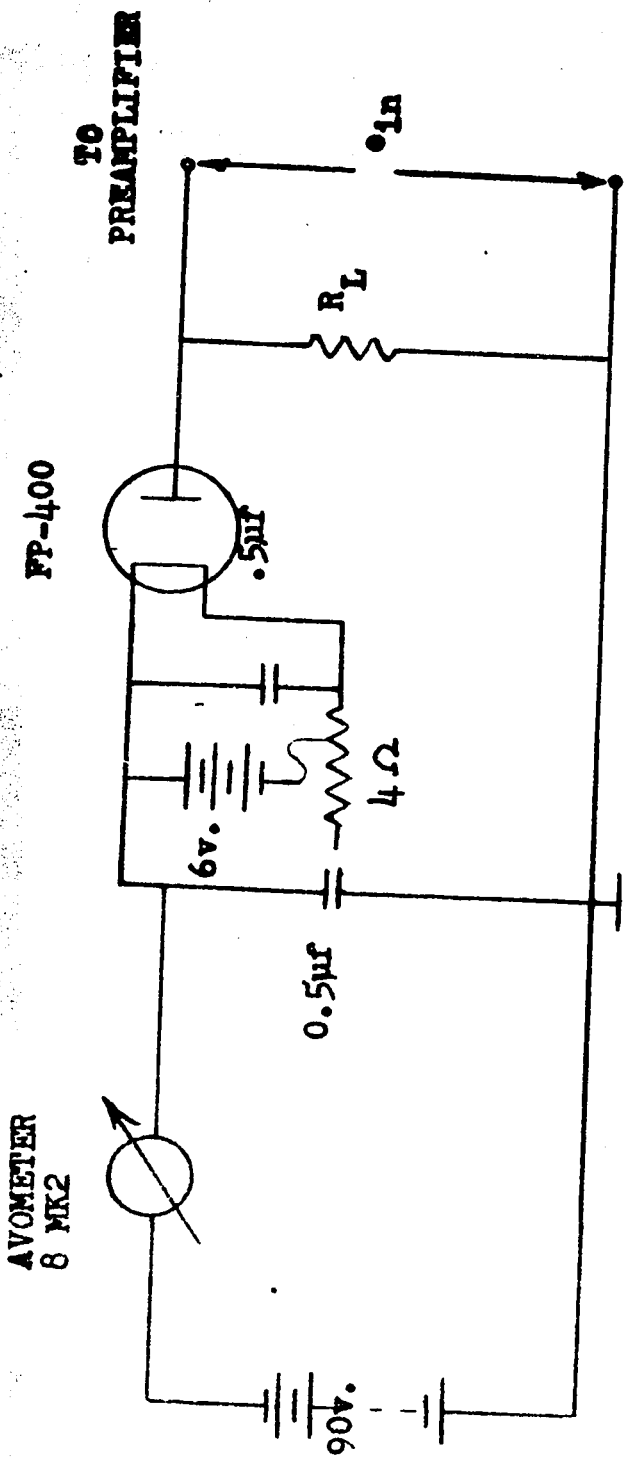

FIGURE 4.17

SATURATED-DIODE NOISE GENERATOR

vacuum tube diode was used (figure 4.17). A saturated vacuum tube diode may be represented[11] by a noise free diode in parallel with a noise current generator of mean square value,

$$\overline{i^2} = 2qIdf \qquad (4.18)$$

where q is the electronic charge, I the d.c plate current of the diode and df the bandwidth of interest.

The mean square noise voltage at the input to the preamplifier is that across the load resistor R_L (figure 4.17) and is given by

$$\overline{e_{in}^2} = 2qIR^2df + 4kTR\,df \qquad (4.19)$$

where k is Boltzmann constant and T is temperature in degrees Kelvin. The second term on the right hand side of (4.19) is the contribution due to thermal noise of the load resistor.

The plate current I was varied by changing the filament temperature of the noise diode: in this way, the input noise-voltage to the preamplifier (e_{in}) was varied and a calibration curve (figure 4.20) was prepared by plotting e_{in} versus the output from the noise amplifier. The curve was prepared for values of input ranging from 10mμv to 0.9μv, the range of noise voltages through which measurements were to be made (cf. sec. 2.1).

The calibration curve was checked using two different

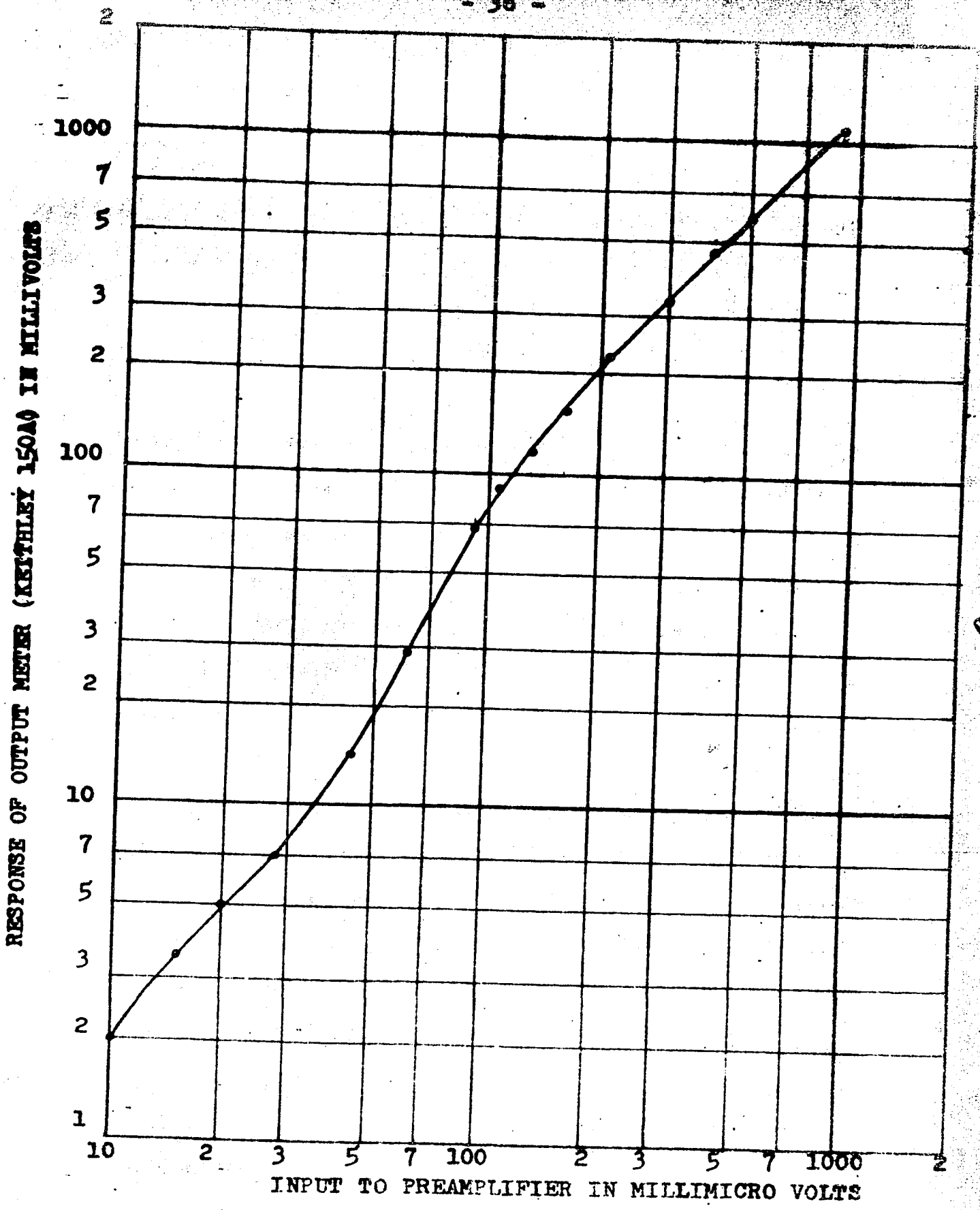

FIGURE 4.20

GAIN CALIBRATION CURVE OF NOISE-AMPLIFIER

diodes of the same type: FP-400[d]. The results from these two tubes were indistinguishable. It was estimated that measurements based on this calibration curve were of better than 5% accuracy.

---

d) The FP-400 manufactured by General Electric Co., is specially constructed for the study of electrical discharges in high vacuum, in particular, the relation between temperature and electron emission. This tube has good saturation properties being built with a pure tungsten filament which is electrically and chemically more robust than other commonly used filament materials. Pure tungsten withstands positive ion bombardment better than other filament materials, and approaches saturation more closely than other cathodes (the work function remains relatively constant with increasing electric field i.e. Schottky's effect is small). In addition, whereas most diodes are designed to operate in the space charge region, the FP-400 is constructed for the large power dissipation required in the saturated region. Because of these reasons, the FP-400 is suitable for use as a noise diode.

PART II

EXPERIMENTAL RESULTS AND CONCLUSIONS

CHAPTER 5: RESULTS

5.1 Description of the Samples

The samples used in this experiment were Philco 2N393 germanium transistors (p-n-p, micro-alloy), which were chosen because :

1) Transistors provided two junctions for approximately the same cost as one diode.

2) For these junctions, the complex portion of the small signal a-c impedance was negligible[a], which greatly simplified the measurement of the junction impedance.

---

a) This is a result of the process of micro-alloying used in the fabrication of the 2N393 transistors. The base-region is prepared by directing a stream of acid etch to each side of an n-type germanium wafer, etching the wafer down to size. This process gives accurately controlled narrow base regions, the thickness being measured by infra-red ray absorption. Included in the jet stream is cadmium in solution, and by passing an electric current through the stream, very small cadmium dots are electroplated to the wafer. The emitter dot is later alloyed.

The narrow base regions and carefully controlled small junction areas (junction capacitance is proportional

3) A large junction area is liable to result in an undulating[b] junction with the noise properties varying from junction to junction. The micro-alloy junction had a small area (diameter 0.0075 inches) and was therefore more likely to have a plane junction.

4) The overall size of the 2N393 was suitable for insertion into the narrow neck of the liquid helium vessels (see figure 4.1), thereby eliminating the use of a cryostat.

5.2 Total Noise Measured Across the Terminals of the Junction

As a considerable amount of work had been done on noise in p-n junctions at low current densities,[3,5,12,13] and

---foot note cont'd

to the junction area) result in good high frequency performance of the 2N393 transistor. The 2N393 is an all purpose high frequency transistor with particular application to switching circuits up to 50 mc.

The junction capacitance was measured to be less than 10μμf, which may be neglected when junction resistances ranging from 0-1000Ω are considered. It is therefore justifiable to refer to the small signal a-c impedance of the junction as the incremental resistance.

b) Undulating in a cross-section taken about any diameter.

very little (as far as I know one published paper[14] on experimental work) at high current densities (see sec. 5.5), emphasis was placed on noise measurements at high current densities. Currents from 10nA to 10mA were used with a junction area of 44.2 x 10^{-6} sq. inches. This gave current densities ranging from 0.226 - 226 amps per sq. inch.

Figure 5.1 shows a typical set of curves for the total noise measured across the terminals of the collector-base junction of the 2N393 transistor as a function of bias current at the temperatures of 4.2°K, 80°K and 300°K.

5.3 Incremental Resistance Measurements

The incremental resistance of the junction was measured under the same conditions as those of the noise measurements, and the values of incremental resistance corresponding to the noise measurements of figure 5.1 are shown in figure 5.2. From these curves of incremental resistance versus bias current the extrinsic base resistance[c] of the sample was deduced. Shockley's equation[d] describing the flow of current

---

c) The extrinsic base resistance is the resistance of the bulk material outside of the junction.

d) This equation was derived for a simplified one dimensional model of a p-n junction. See W. Shockley "Theory of p-n Junctions", Bell Syst. Tech. J. 28, 435-489 (1949).

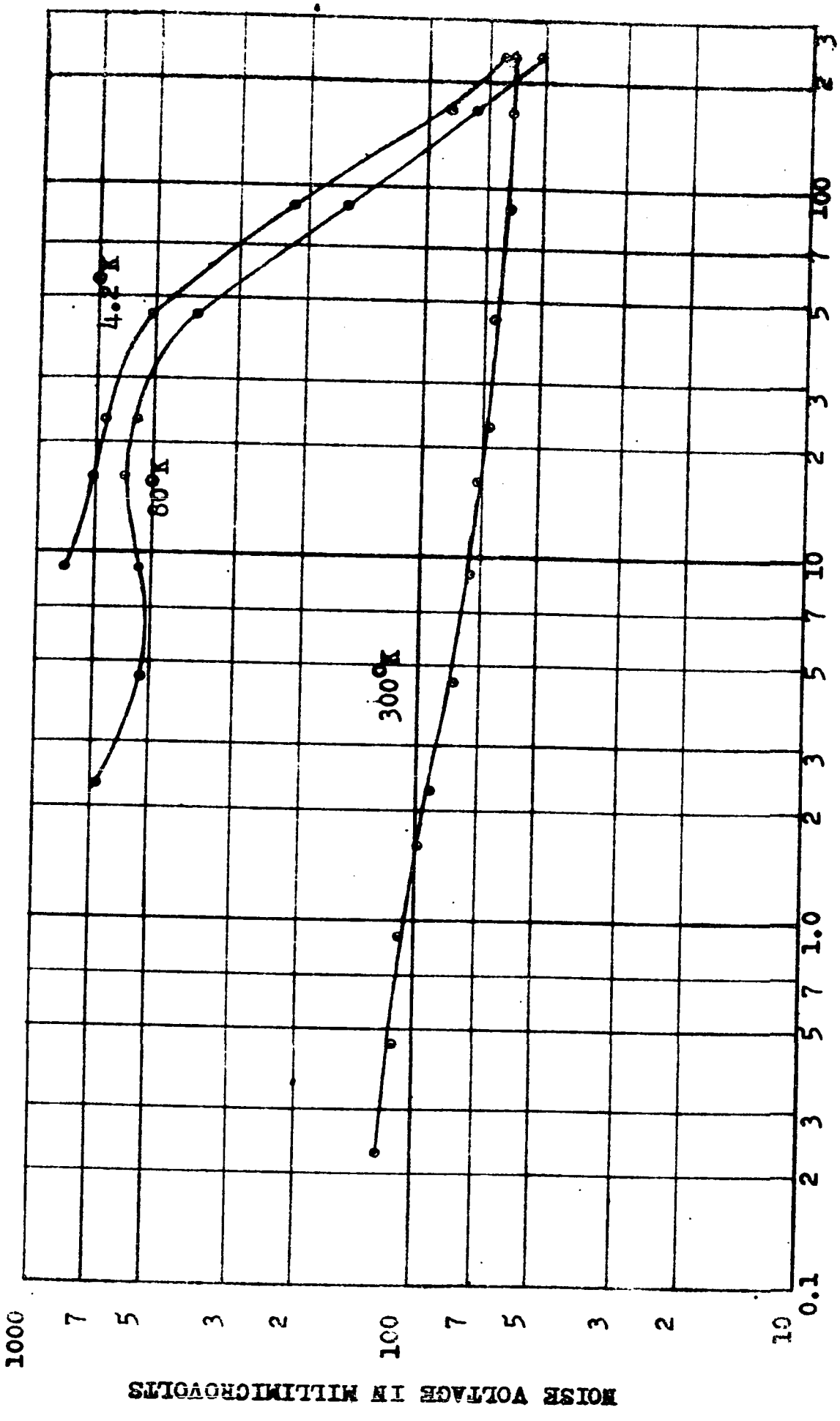

FIGURE 5.1

TOTAL NOISE MEASURED ACROSS COLL.-BASE TERMINALS OF PHILCO 2N393 TRANSISTORS AS A FUNCTION OF CURRENT DENSITY

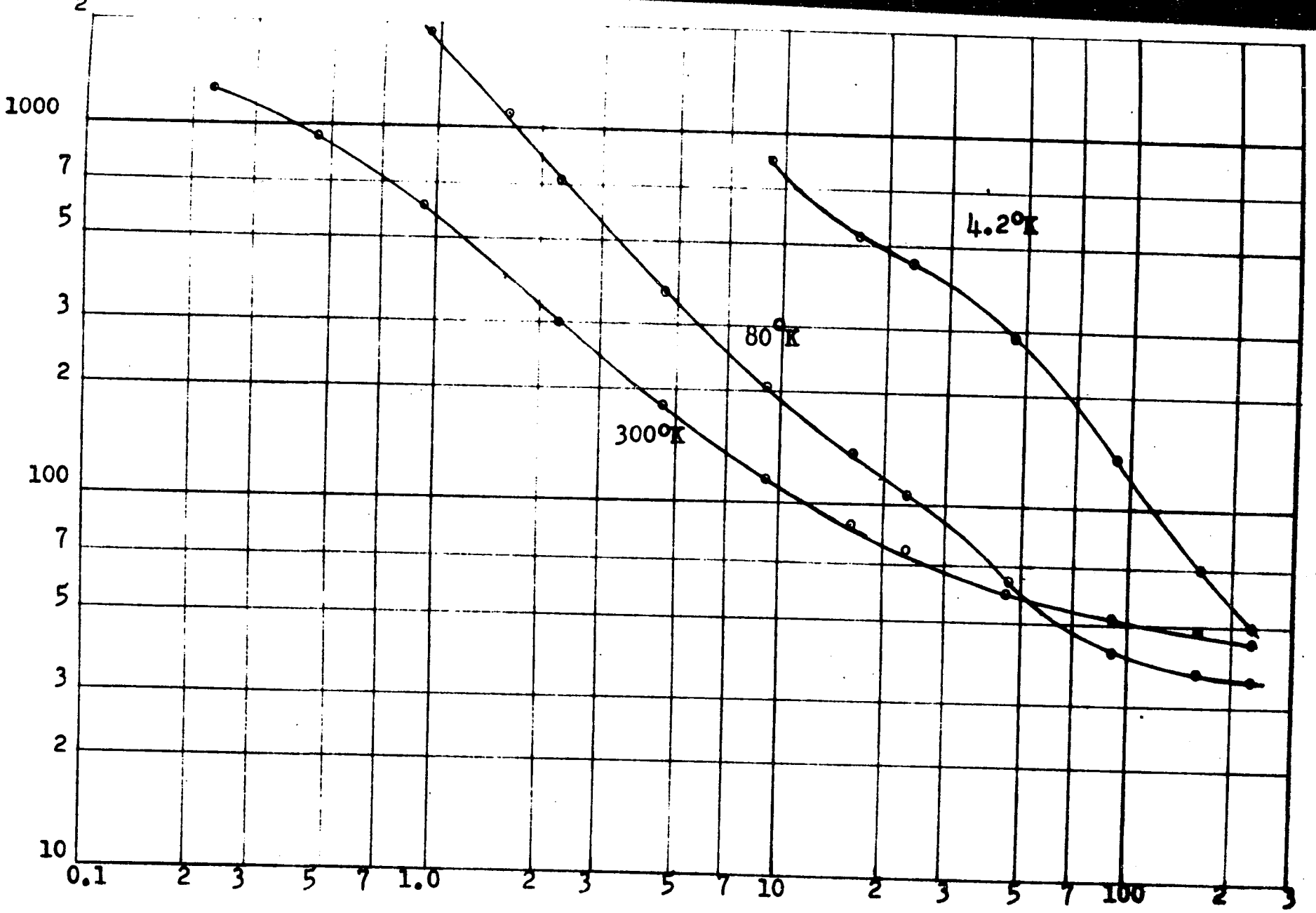

FIGURE 5.2

INCREMENTAL RESISTANCE OF SAMPLE JUNCTION AS A FUNCTION OF CURRENT DENSITY

in a p-n junction is

$$I = I_o \left(e^{\frac{qv}{kT}} - 1\right) \qquad (5.3)$$

where I_o is the reverse saturation current and v is the voltage applied to the junction. Differentiating with respect to v gives

$$\frac{dI}{dv} = \frac{q}{kT} I_o e^{\frac{qv}{kT}} = \frac{q}{kT}(I+I_o)$$

$$= \frac{q}{kT} I \quad \text{for } I \gg I_o$$

$$\therefore R = \frac{dv}{dI} = \frac{kT}{qI} \qquad (5.4)$$

where R is the incremental resistance of the junction.

At low currents, therefore, the measured incremental resistance is mainly due to the potential barrier existing at the junction, while at high currents, the measured resistance tends to the value of the extrinsic base resistance. For the junction, whose noise properties are shown in figure 5.1, the extrinsic base resistance was 23, 35 and 44 Ω at 4.2°K, 80°K and 300°K respectively.

5.4 Noise of the Junction

Full Nyquist noise was assumed[e] for the extrinsic

---

e) This assumption is based on a statement of B. Schneider and M. J. O. Strutt[14], who were using the conclusion

base resistance and this noise was subtracted from the total noise ($4kTdf$ at $300^{\circ}K$ = 74×10^{-18} watts, therefore the mean square value of thermal noise at $300^{\circ}K$ is 33×10^{-16} volts squared). The remaining noise, shown in figure 5.5, was assumed to be generated at the junction and its magnitude will be compared with that predicted by existing theory.

foot note cont'd

of W. Guggenbuehl's M. S. thesis, Swiss Federal Institute of Technology, Zurich, Switzerland.

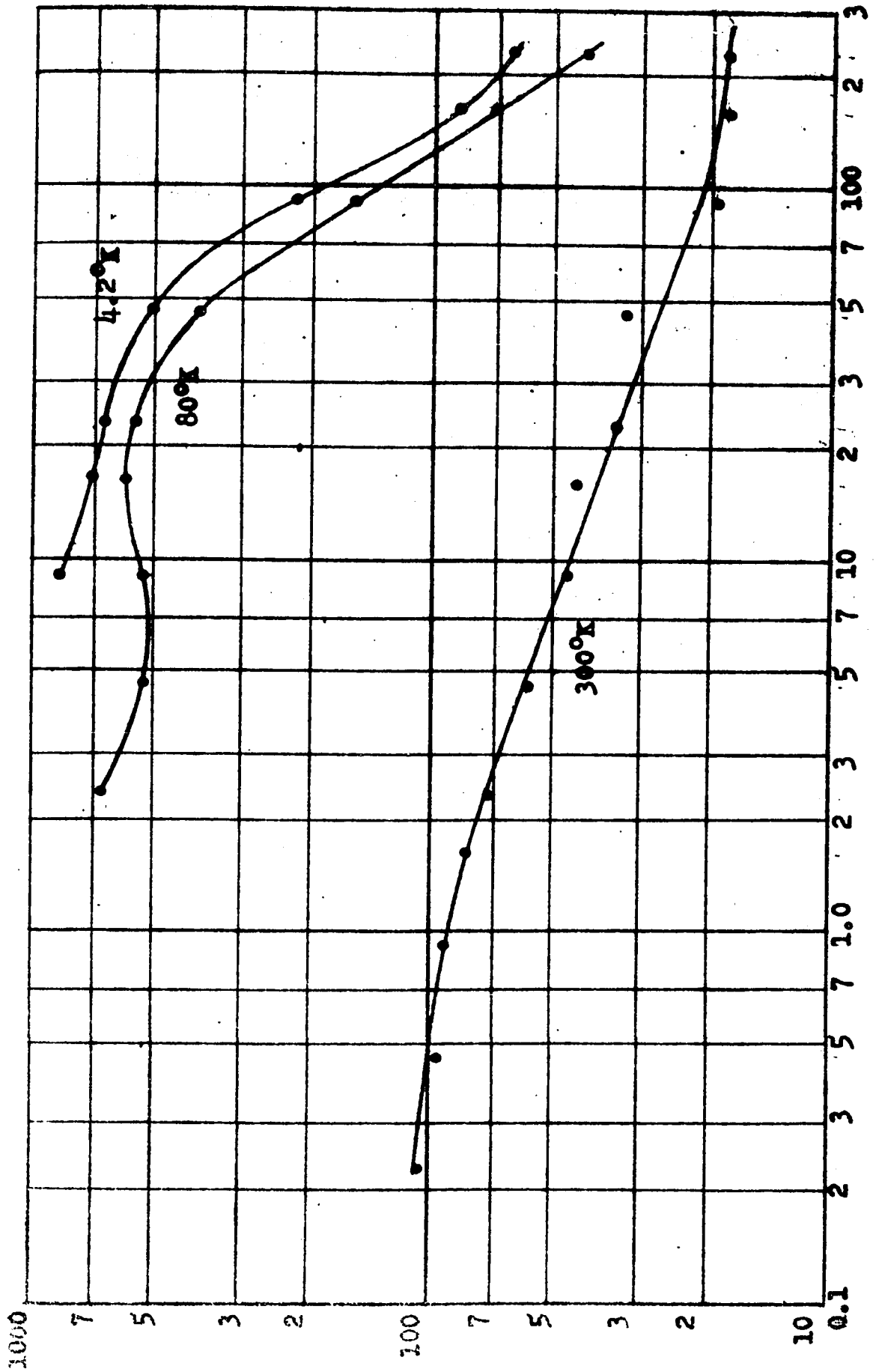

CURRENT DENSITY IN AMPS PER SQUARE INCH.

FIGURE 5.5

JUNCTION NOISE AS A FUNCTION OF CURRENT DENSITY
(TOTAL NOISE MEASURED MINUS THERMAL NOISE).

CHAPTER 6: DISCUSSION OF RESULTS

6.1 Results Expected from Existing Theory

At low current densities, good coincidence has been obtained between experimental and calculated results by other workers[3,5] in this field. In those experiments, van der Ziel's[4] noise equivalent circuit (figure 6.1) for a p-n junction was used to obtain the calculated results. As shown in figure 6.1, this equivalent circuit is a noise-free junction of admittance Y in parallel with a noise current generator of mean square value

$$\overline{i^2} = \left[4kTRe(Y) - 2qI\right] df \qquad (6.2)$$

where Re(Y) is the real part of the junction admittance.

The above equation was derived on the assumptions:[4] i) that the noise is attributed to a series of random and independent crossings of the junction by current carriers and ii) that traps present in the space charge region have no effect on diffusion. Thermal noise due to the contact resistance and the extrinsic base resistance is excluded from (6.2) but is represented in figure 6.1 by a resistor r, equal to the contact resistance plus the extrinsic base resistance showing full Nyquist noise.

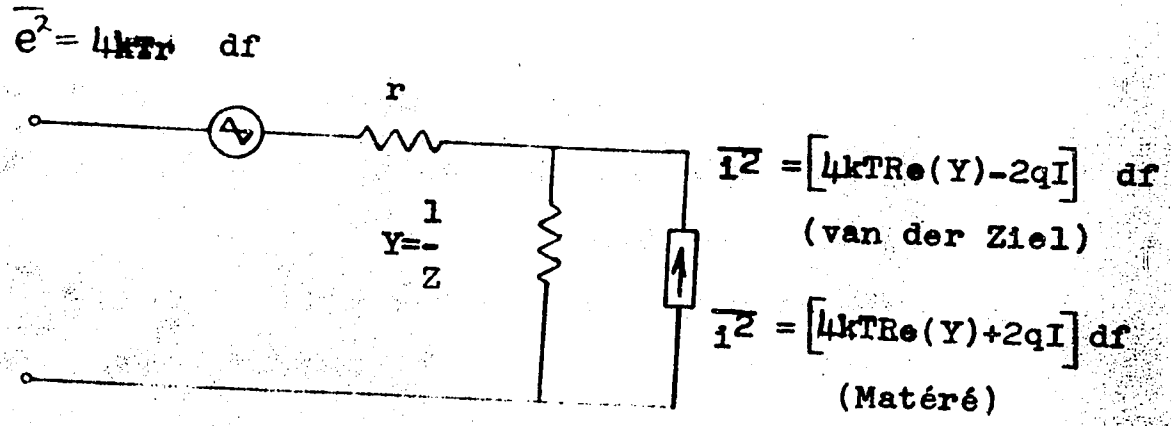

FIGURE 6.1

van der Ziel's low frequency model for the noise of a p-n junction. Mataré's expression for the current source is also indicated.

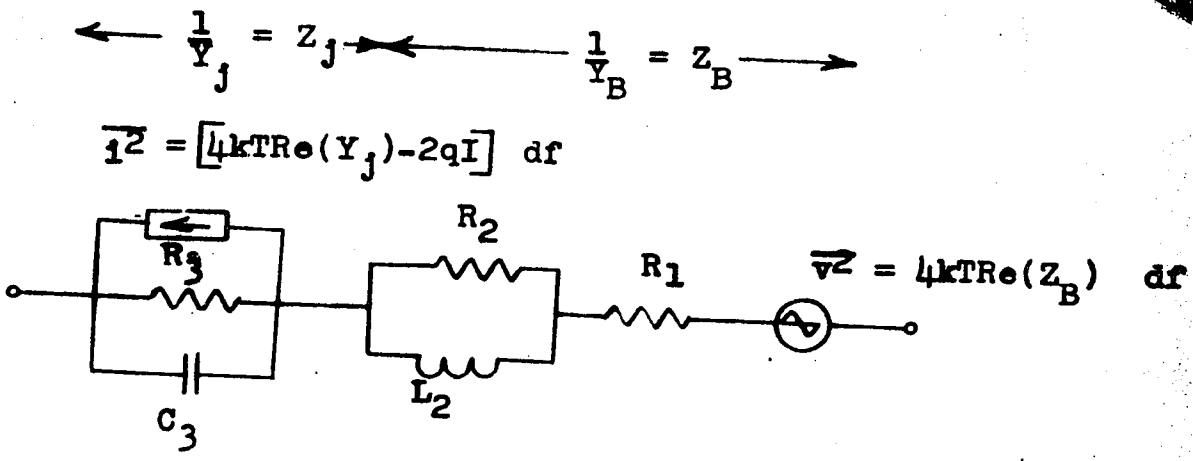

FIGURE 6.3

Noise equivalent circuit of Schneider and Strutt for a p-n junction at high current densities.

At high current densities[a], both the minority and majority carrier densities increase by several orders of magnitude above their equilibrium values i.e. above the concentration of carriers found in the semiconductor material in the absence of an external field. Under these conditions, it was found[6] that equation 6.2 no longer predicts the noise properties of a p-n junction.

Two postulates were put forward to explain the deviation from (6.2) at high current densities. A. van der Ziel[15] expects a considerable space charge outside the junction causing a correlation between carriers thus violating one of the assumptions on which (6.2) is based (independent crossings of the junction by carriers). W. Guggenbuehl and M. J. O. Strutt,[3] on the other hand, expect that the number of carriers drawn into the junction might be influenced by voltage variations, which were caused by variations of the carrier concentration outside the junction. Neither of these postulates has been verified experimentally nor proven theoretically.

---

a) When a large field is applied to a p-n junction, minority carriers are injected into the base region from the emitter. These injected carriers tend to create a space charge; therefore, majority carriers enter from the base lead to neutralise the charge, causing an overall increase in carrier concentration. "High Current densities" or "high level current injection" implies the condition when the concentration of injected carriers becomes comparable to or greater than the impurity concentration.

B. Schneider and M. J. O. Strutt[14] performed experiments on the noise in p-n junctions at high current densities and assumed both the above effects to be trivial. They calculated the expected noise from the junction by applying equation 6.2 to a new equivalent circuit (figure 6.3) which included an inductor as well as resistors and a capacitor. Z_B in figure 6.3 represents the impedance of the semiconductor material outside the space charge region with its noise given by Nyquist's relation.

$$\overline{V_n^2} = 4kTRe(Z_B)\ df$$

H. F. Mataré[16] has suggested a different expression for the noise current generator of figure 6.1 under conditions of high current densities. By considering an equivalent network for the barrier with an I-V relationship of the form

$$I = k_1 V^n + k_2 V$$

where k's are constants, the mean square noise current of (6.1) becomes

$$\overline{i^2} = \left[4kTRe(Y) + 2qI\right] df \qquad (6.4)$$

Since, as was shown in section 5.1, the impedance of the junction was mainly resistive, the model of figure 6.1 was used to calculate the expected noise from the junction. Using the experimentally found values for Re(Y), the second term in (6.2) was greater than the first for conditions at $4.2^{\circ}K$ and $80^{\circ}K$, which led to meaningless results. At these

temperatures, therefore, equation 6.4 was used to calculate the noise of the junction. Figure 6.5 shows experimental results together with results calculated both by (6.2) and (6.4) at 300°K. Figures 6.6 and 6.7 show experimental and calculated results at 4.2°K and 80°K respectively, the calculated results being obtained from equation 6.4.

6.2 Comparison of Experimental and Calculated Results

As shown in figure 6.5, van der Ziel's theory (equation 6.2) gave results which were in better agreement with experimental results at 300°K than results calculated by Mataré's theory (equation 6.4). At 4.2°K and 80°K, however, results calculated from van der Ziel's theory were meaningless, while results calculated from Mataré's theory showed good agreement ($\pm$ 40%) with experimental results at 4.2°K (figure 6.6) and poorer agreement at 80°K (figure 6.7)

It seems therefore that Mataré's theory approximates more closely the noise properties of p-n junctions at low temperatures and high current densities. This was to be expected since van der Ziel's theory was based on the non-interaction of current carriers; and the abundance of carriers at high current densities removes this condition.

Both theories mentioned above neglect G-R noise, the noise caused by the fluctuation of generation and recombination rates in the bulk material. It is possible that fluctuations

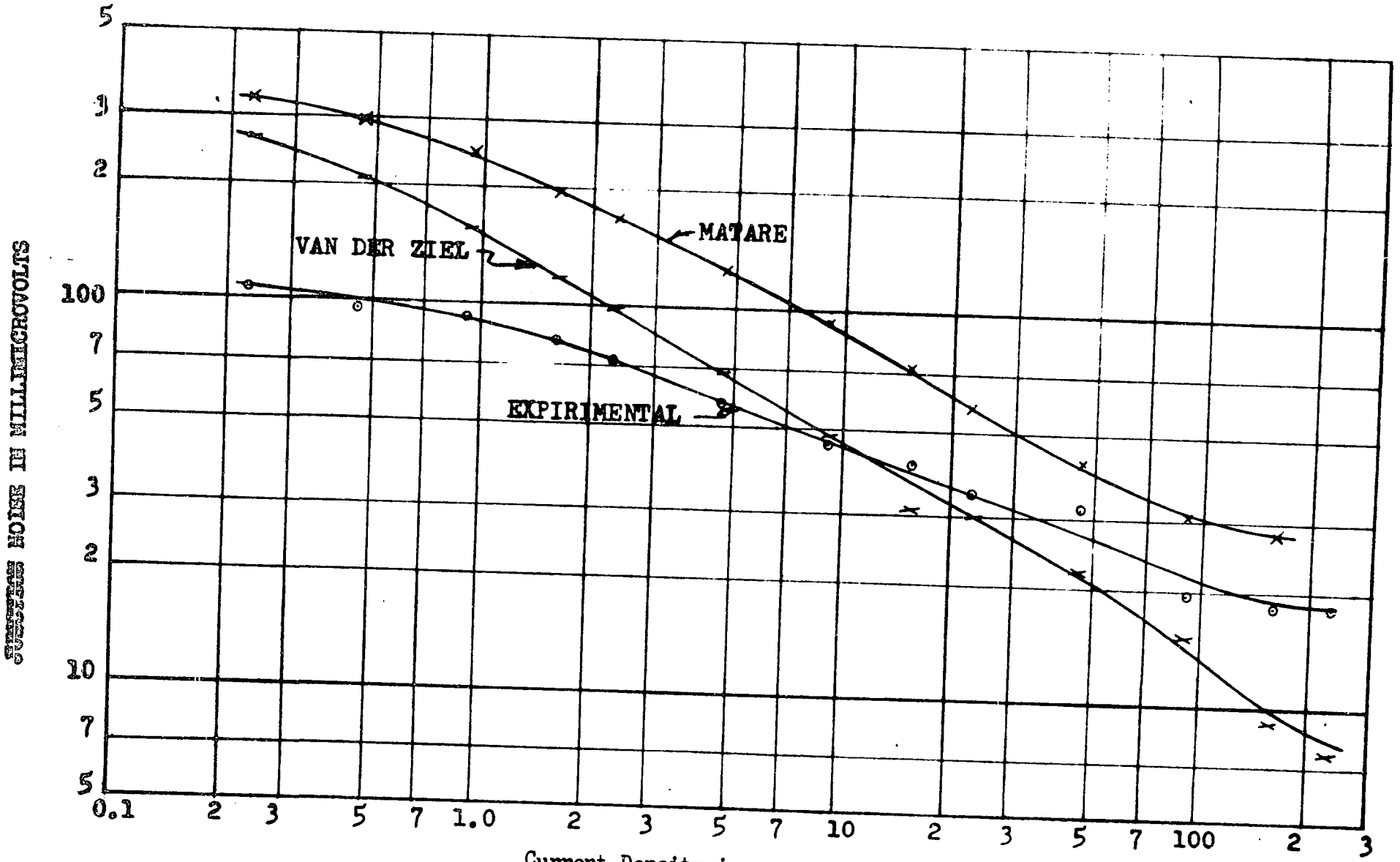

FIGURE 6.5

JUNCTION NOISE AT 300°K COMPARED WITH MATARE'S AND VAN DER ZIEL'S THEORIES.

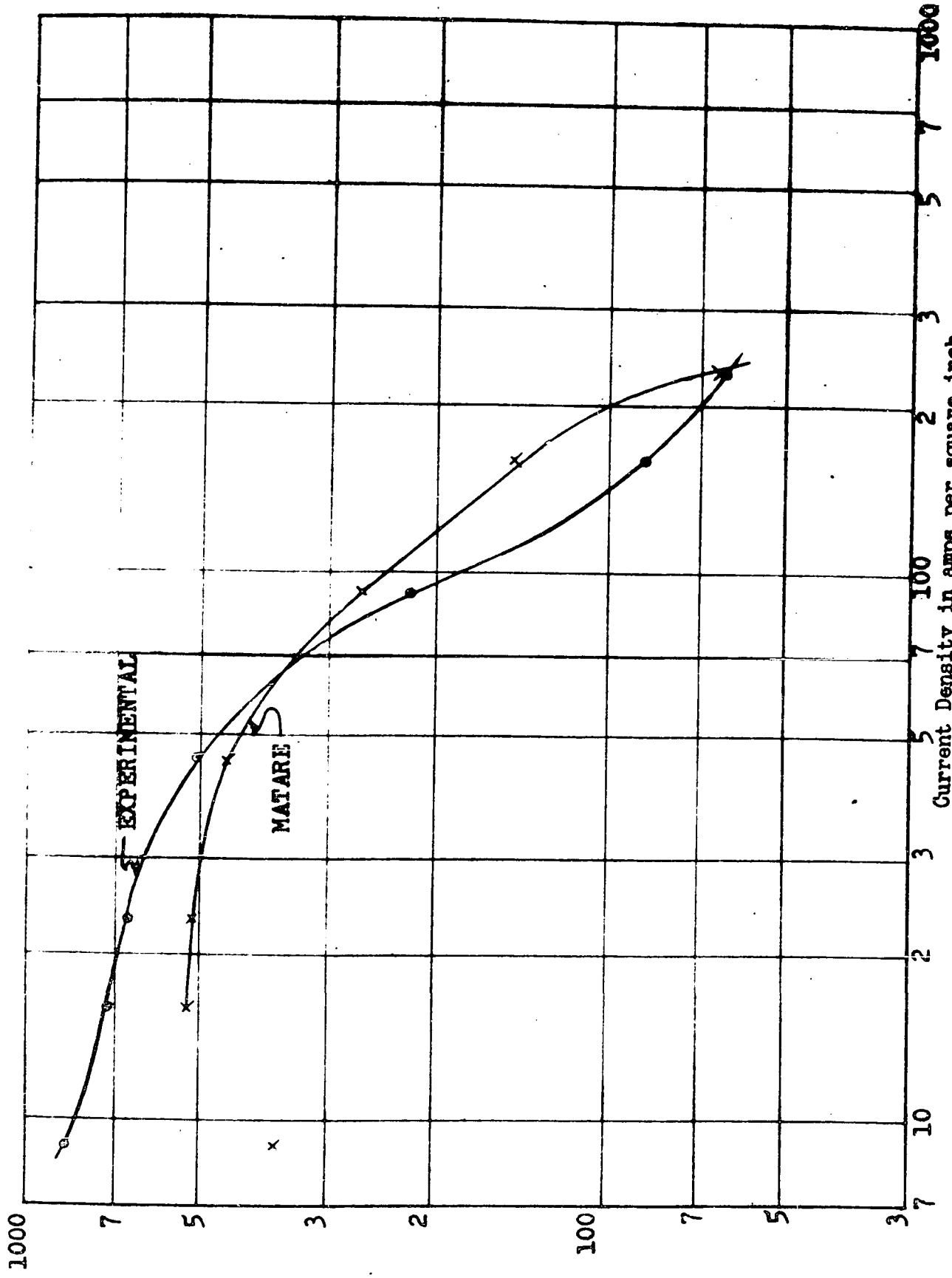

FIGURE 6.6

JUNCTION NOISE AT 4.2°K COMPARED WITH MATARE'S THEORY

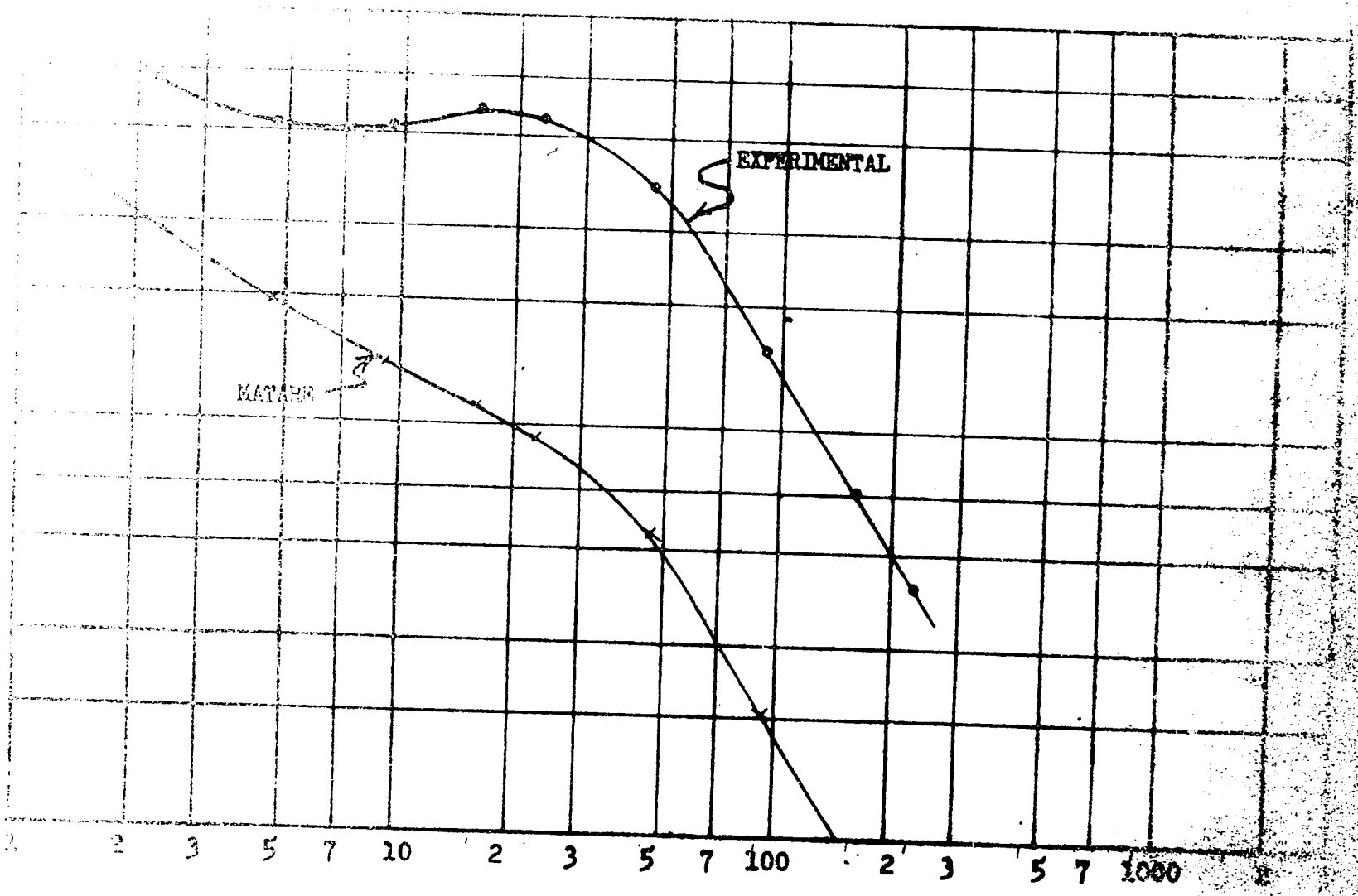

CURRENT DENSITY IN AMPS PER SQUARE INCH

FIGURE 6.7

JUNCTION NOISE AT 80°K COMPARED WITH MATARE'S THEORY

in the G-R noise level might have caused the deviation between experiment and theory. This suggestion is in some way related to the postulate of Guggenbuehl and Strutt mentioned in section 6.1.

CONCLUSION

Experimental apparatus was built to measure the noise voltage developed across the terminals of a p-n junction biased in the forward direction, and measurements of this noise were made as a function of diode current at the temperatures $4.2^{\circ}K$, $80^{\circ}K$ and $300^{\circ}K$. At the operating frequency (1.15 mc) flicker noise was assumed negligible and thermal noise due to the extrinsic base resistance was subtracted from the total noise leaving the noise of the junction.

The resulting junction noise showed rough agreement with van der Ziel's theory at $300^{\circ}K$ and fairly good agreement with Matarè's theory at $4.2^{\circ}K$. I suspect that the disagreement between theory and experiment at $80^{\circ}K$, and even that at $4.2^{\circ}K$ and $300^{\circ}K$, was due to variations in G-R noise level. The p-n junction is a microscopically complex device and before its noise properties are thoroughly understood, more research will be necessary on bulk semiconductors, in particular the variations of G-R noise with current and temperature. It is expected that research will be conducted in this direction in the near future.

APPENDIX 1

Three ways of connecting the sample p-n junction to the preamplifier are discussed, the voltage transfer ratios and the noise factors of the connecting circuits are derived and numerical values are substituted into the expressions for comparison of the different connections. The comparison is illustrated in graphical form in figure A.2. Figure 4.2, showing the different forms of connection, is redrawn in figure A.1, a form more suitable for circuit analysis.

1) Direct Connection

Direct connection of the p-n junction to the amplifier constitutes a low pass filter (figure A.1a), and is therefore limited to relatively low frequencies.

The voltage transfer ratio of the circuit

$$G_1 = \left| \frac{Z_o}{Z_{in}} \right|$$

$$Z_o = \frac{R_s - j R_s^2 \omega C}{\omega^2 C^2 R_s^2 + 1}$$

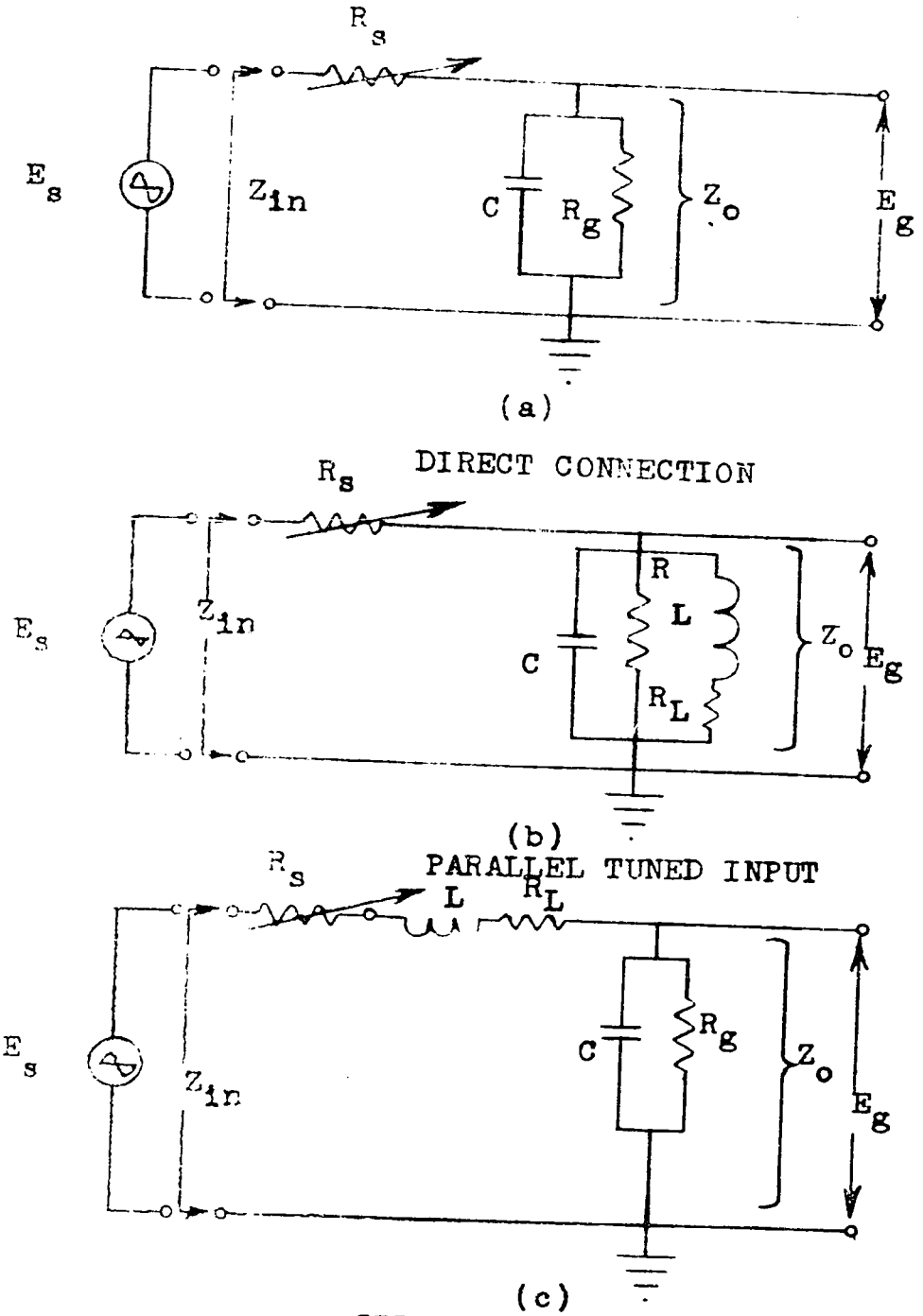

FIGURE A.1

THREE WAYS OF CONNECTING THE P-N JUNCTION TO THE PREAMPLIFIER

$$Z_{in} = R_s + \frac{R_g - jR_g^2\omega C}{\omega^2 C^2 R_g^2 + 1}$$

$$\therefore G_1 = \left| \frac{R_g - jR_g^2\omega C}{R_s(\omega^2 C^2 R_g^2 + 1) + R_g - jR_g^2\omega C} \right| \qquad (1)$$

The noise factor

$$N_1 = 1 + \frac{N_{R_g}}{N_{R_s}} \qquad (a)$$

$$= 1 + \frac{4kTR_g\,df}{4kTR_s\,df\,G_1^2} \left[\frac{R_s - jR_s^2\omega C}{\omega^2 C^2 R_s^2 + 1} \Big/ R_g + \frac{R_g - jR_g^2\omega C}{\omega^2 C^2 R_s^2 + 1} \right]^2$$

$$= 1 + \frac{R_g}{G_1^2 R_s} \left[\frac{R_s - jR_s^2\omega C}{R_g(\omega^2 C^2 R_s^2 + 1) R_s - jR_s^2\omega C} \right]^2 \qquad (2)$$

2) <u>Parallel Tuned Connection</u>

The parallel tuned input (figure A.1b) is the most practical form of connection as it allows measurements to be made at any frequency with both the voltage transfer ratio and the noise factor close to unity.

---

a) N_{R_g} is the noise power originating in the resistance R_g due to thermal noise.

The gain

$$G_2 = \frac{Z_o}{Z_{in}}$$

At resonance $Z_o = \dfrac{R_g L}{CR_L(R_g + L/CR_g)}$

$$\therefore G_2 = \frac{LR_g}{L + CR_L R_s\left[R_s + \dfrac{LR_g}{L+CR_g R_L}\right]} = \frac{LR_g}{R_s(L+CR_L R_g)+LR_g} \quad (3)$$

The noise factor

$$N_2 = 1 + \frac{N_{R_L}}{N_{R_s}} + \frac{N_{R_g}}{N_{R_s}}$$

$$= 1 + \frac{R_g}{R_s G_2^2}\left[\frac{\dfrac{LR_s}{L+CR_L R_s}}{R_s + \dfrac{LR_s}{L+CR_L R_s}}\right]^2 + \frac{R_L}{R_s G_2^2}$$

$$\times \left[\frac{\dfrac{R_g R_s}{R_g+R_s} - j\dfrac{R_g^2 R_s^2 \omega C}{(R_g+R_s)^2}}{\omega L\left(\dfrac{\omega^2 C^2 R_g^2 R_s^2}{(R_g+R_s)^2}+1\right)+\dfrac{R_g R_s}{R_g+R_s} - j\dfrac{R_g^2 R_s^2 \omega C}{(R_g+R_s)^2}}\right]^2$$

$$= 1 + \frac{R_g}{R_s G_2^2}\left[\frac{1}{\dfrac{R_s(L+CR_L R_s)}{LR_s}+1}\right]^2 + \frac{R_L}{R_s G_2^2}\left[\frac{R_s - jR_s^2\omega C}{\omega L(\omega^2 C^2 R_s^2+1)+R_s - jR_s^2\omega C}\right]^2 \quad (4)$$

3) The series tuned connection

The series tuned input (figure A.1c) give a voltage transfer ratio greater than unity and is therefore useful where the amplifier does not have sufficient gain. At first sight this may seem to be very attractive but if the bandwidth must be wide (in order that the overall bandwidth of the equipment be constant with respect to changes in the source inpedance, the input bandwidth must be several times larger than any of the tuned stages which follow) the gain must be much samller than the maximum gain.

Since the series tuned connection has a low noise factor, it may also reduce the noise factor of a noisy amplifier.

The gain of the network

$$G_3 = \left| \frac{Z_o}{Z_{in}} \right|$$

$$Z_{in} = R_s + R_L + \frac{R_g}{\omega^2 C^2 R_g^2 + 1} + j\left[\omega L - \frac{\omega C R_g^2}{\omega^2 C^2 R_g^2 + 1}\right]$$

at resonance

$$\omega_o L - \frac{\omega_o C R_g^2}{\omega_o^2 C^2 R_g^2 + 1} = 0$$

$$\therefore Z_{in} = R_s + R_L + \frac{R_g}{\omega_o^2 C^2 R_g^2 + 1}$$

$$\therefore G_3 = \left| \frac{R_g - jR_g^2\omega_o C}{(R_s+R_L)(\omega_o^2 C^2 R_g^2+1)+R_g} \right| \qquad (5)$$

The noise factor

$$N_2 = 1 + \frac{N_{R_L}}{N_{R_s}} + \frac{N_{R_g}}{N_{R_s}}$$

$$= 1 + \frac{4kTR_L\ df\ G_2^2}{4kTR_s\ df\ G_2^2} + \frac{4kTR_g\ df\ L^2}{\left[R_g + \frac{L}{C(R_L+R_s)}\right]^2 C^2R_g^2\ (4kTR_s\ df\ G_2^2)}$$

$$= 1 + \frac{R_L}{R_s} + \frac{L^2(R_L+R_s^2)^2}{R_sR_g} \frac{\left[(R_s+R_L)(\omega_o^2C^2R_g^2+1)+R_g\right]^2}{\left[CR_g(R_L+R_s)+L\right]^2 \left[R_g - jR_g^2\omega_o C\right]^2} \qquad (6)$$

For a comparison of the different forms of connection, the following values were substituted into equations (1) to (6) and the results shown in graphical form (figure A.2)

f_o	= 1 mc	L	= 0.125 mh
C	= 200μμf	R_L	= 6.3 Ω
R_g	= 300 KΩ		

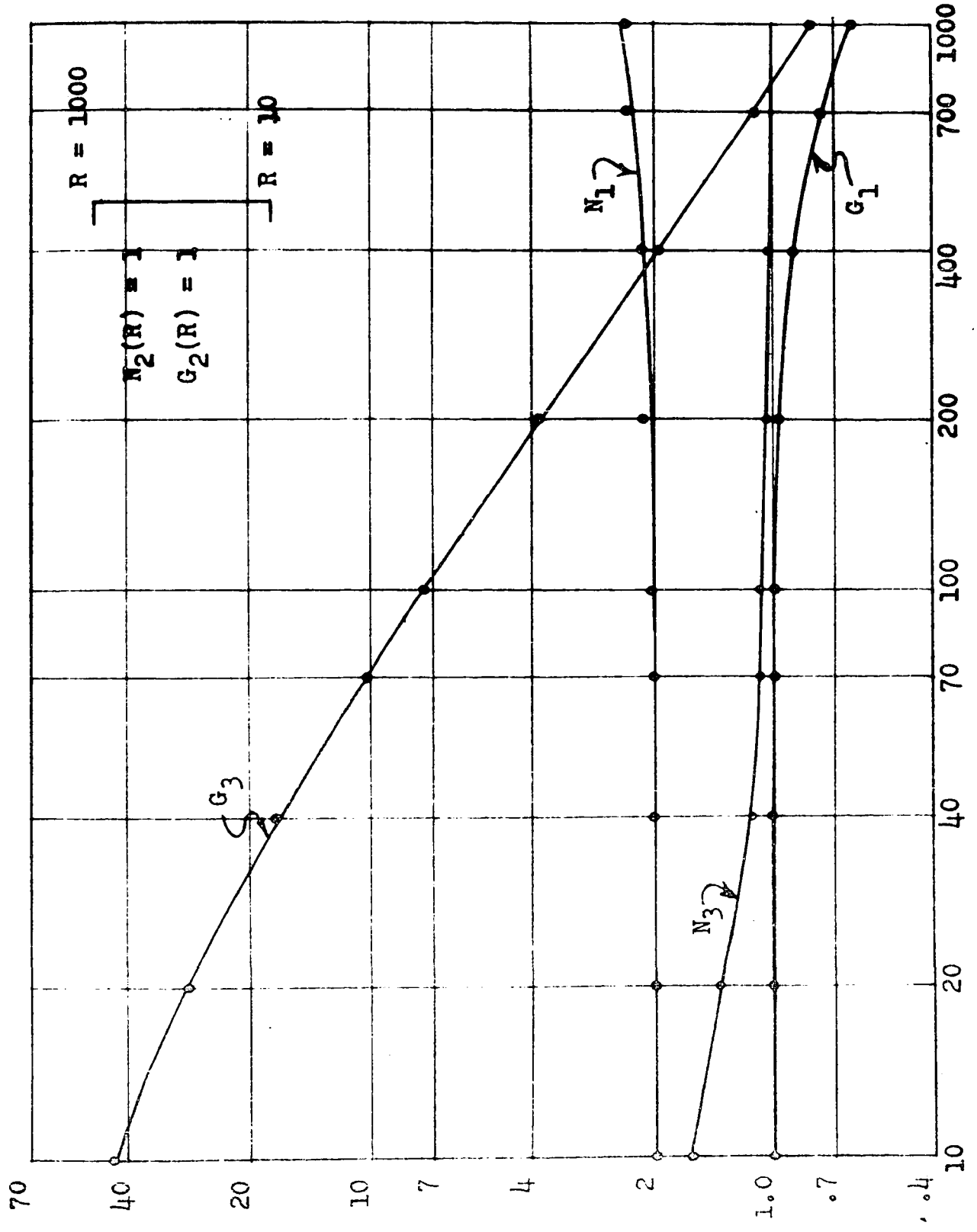

FIGURE A.2

COMPARISON OF THE VOLTAGE TRANSFER RATIOS AND NOISE FACTORS FOR THE THREE FORMS OF CONNECTING THE P-N JUNCTION TO THE PREAMPLIFIER

LIST OF REFERENCES

1. O. Celinski, "Spontaneous Fluctuations of Electricity", MSc. thesis, Physics Dept., University of Ottawa (1961)
2. J. W. Englund, "Noise Considerations for P-N-P Junction Transistors", Transistor I, RCA Laboratories, Princeton, N.J.
3. W. Guggenbuehl and M. J. O. Strutt, "Theory and Expirement on Shot Noise in Semiconductor Junction Diodes and Transistors", Proc. IRE, 45, 839-854; May 1957.
4. A. van der Ziel, "Fluctuation Phenomena in Semi-Conductors", Semi-Conductor Monograph (1959).
5. A. van der Ziel, "Theory of Shot Noise in Junction Diodes and Junction Transistors", Proc. IRE, 43, 1639-1646; November 1955.
6. B. Schneider and M. J. O. Strutt, "Theory and Experiments on Shot Noise in Silicon P-N Junction Diodes and Transistors", Proc. IRE, 47, 546-554; April 1959.
7. H. T. Friis, "Noise Figures of Radio Receivers", Proc. IRE, 32, 419-422; July 1944.
8. H. Wallman et al, "A Low-Noise Amplifier" Proc. IRE, 56, 700-708; June 1948.
9. W. R. Bennett, "Electrical Noise", McGraw-Hill Book Company, Inc., N. Y. (1960).

10. A. van der Ziel, "Noise", Prentice-Hall Electrical Engineering Series (1956).

11. J. J. Freeman, "Principles of Noise", John Wiley and Sons, Inc., N. Y.

12. A. van der Ziel, "Shot Noise in Junction Diodes and Transistors", Proc. IRE, 45, 1011; July 1957.

13. A. van der Ziel and A. G. T. Becking, "Theory of Junction Diode and Junction Transistor Noise", Proc. IRE, 46, 589-594; March 1958.

14. B. Schneider and M. J. O. Strutt, "Shot and Thermal Noise in Germanium and Silicon Transistors at High-Level Current Injections", Proc. IRE, 48, 1731-1739; Oct. 1960.

15. A. van der Ziel, "Noise in Junction Transistors", Proc. IRE, 46, 1019-1038; June 1958.

16. H. F. Mataré, "Theory of Diode and Transistor Noise", Proc. IRE, 46, 1964; Dec. 1958.

VITA

Name:	Winston Randolph Samaroo
Born:	Trinidad, The West Indies, Feb. 24, 1934
Educated:	
Primary:	San Fernando E. C. School,
	Trinidad, T. W. I.
Secondary:	Naparima College
	Trinidad, T. W. I.
	Presentation Brothers College
	Trinidad, T. W. I.
University:	McGill University
	Montreal, Canada
Course:	Electrical Engineering (Communications)
Degree:	B. Eng.